Politecnico di Torino

Master of Science Degree in Automotive Engineering
Academic Year 2022/2023
Decembre 2023 Degree Session

Structural Design of Rear Wing of a Formula Student Racing Car

Advisor:
Andrea Tonoli
Co-advisor:
Stefano Favelli

Candidate:
Nicola Erriu

Abstract

This work presents the structural design evolution of a multi-element rear wing for a Formula Student racing car for the 2024 season, with innovations in both structural configuration and production techniques. The analysis initiates with an in-depth examination of the 2021 Rear Wing, featuring CFRP outer shells and a rigid foam inner core – the prior assembly version. Subsequent investigation of the 2022 season test highlights a critical factor in the mainplane failure: improper support attachment positioning. The design of the Rear wing assembly for upcoming season addresses this, incorporating hollow wing elements with a carbon fibre shell in a sandwich structure, complemented by thick rigid foam or honeycomb, depending on the component. Key design objectives include support optimization from both structural and production perspectives, achieving a remarkable 56% weight reduction without the need for milling processes. Additionally, the displacement under a 60 km/h aerodynamic load is maintained below 2mm to preserve aerodynamic performance. The design optimizes manufacturing processes, reducing costs by minimizing machining operations through extensive waterjet cutting. The assembly utilizes a Low-Density High Modulus carbon fibre prepreg and a Carbon Fiber with a Balanced Strength-to-Weight Ratio, whose mechanical properties are determined through in-house tensile tests according to D3039 normative. Structural analysis is conducted using the Finite Element Method with Altair Hypermesh and Optistruct as the solver. An experimental test under static conditions has been conceptualized to establish a correlation between the numerical model and the actual behaviour of the component, which execution is left to future stages of this work. The result is a more efficient overall structure, estimating a 5% weight reduction compared to 2021 while accommodating a 30% increased aerodynamic load. This underscores the heightened efficacy of the hollow sandwich structure solution.

Index

List of Figures

List of Tables

1. Introduction

Squadra Corse PoliTo, established in 2004, is a student team dedicated to competing in the Formula Student championship. This global design competition requires student teams worldwide to design and manufacture a single-seater vehicle in accordance with the technical regulations set by the Society of Automotive Engineers.

The current team vehicle, SC22evo, features a carbon fibre monocoque and an aerodynamic package comprising:

- Front wing
- Sidepods
- Rear wing
- Undertray and diffuser

This work focuses on presenting the structural design of the vehicle's rear wing for the 2024 season, starting with an examination of the current version in use.

Chapter 2 conducts a comprehensive analysis of the 2021 Rear Wing assembly, identifying areas for potential optimization to achieve a more efficient and lightweight structure. Moreover, this chapter explores the circumstances surrounding the mainplane failure observed in a test conducted during the 2022 season.

Chapter 3 explores the design decisions for the new wing assembly, detailing the constituent components, the structural modeling approach for Finite Element Method (FEM) analysis, and the chosen load cases for investigating and dimensioning the structure against various scenarios.

Chapter 4 focuses on characterizing the composite material employed in Wing component production through tensile tests, especially considering the absence of datasheets accompanying the materials provided to the team.

Chapter 5 describes the design of an experimental test aimed at establishing a correlation between numerical results and real component behavior. This correlation facilitates a more precise dimensioning of the component through numerical modeling.

Chapter 6 summarizes the results obtained from simulations, outlining the final dimensioning of the components and the decisions leading to these outcomes.

Chapter 7 Offers a concise overview of the results derived from the aforementioned chapters, providing a cohesive summary of the work conducted.

Figure 1. SC22 at Varano track

2. Analysis of Rear Wing 2022

In this chapter, we will conduct a thorough analysis of the most recent version of the rear wing, serving as the foundation for the design of its upcoming version. Special focus will be given to identifying and addressing any weaknesses in the existing design for improvement in the subsequent release.
The rear wing utilized in the SC22evo, the 2023 season car, is the one constructed in 2021. It comprises multiple elements, including a mainplane and three flaps.
In the 2022 season, a Beam element was introduced to improve the aerodynamic performance of the wing. Additionally, slight modifications were made to the endplate geometry to achieve greater clearance from the regulatory limitations regarding the visibility of the TSAL (Tractive System Active Light).
The layup details for the various elements of the 2021 Wing are provided in the table below.

COMPONENTS	Nº PLIES	TYPE	CORE	LAYUP
Flap 1	7	TEXTREME	ROHACELL IG31	0º-90º
Flap 2	3	TEXTREME	ROHACELL IG31	0º-90º
Flap 3	4	TEXTREME	ROHACELL IG31	0º-90º
Endplates	2	TEXTREME	ROHACELL IG31	0º-90º
Main	3	T1100	ROHACELL IG31	0º-45º
Supports	10	T1100	ROHACELL IG31	0º-45º

Table 1. Rear Wing 2021 laminate configuration

2.1 Support Geometry

The geometry of the support was selected based on its influence on aerodynamic performance. The section of the support in contact with the mainplane features a NACA symmetric profile to minimize wake generation and disturbances to the wing. Consequently, its shape was not optimized for structural purposes, and the material used in it is not efficiently utilized for its primary function. To adhere to the technical requirements outlined in Formula Student regulations, 10 plies of T1100, each with a thickness of 0.23mm, were employed. The overall weight of the entire support assembly (supportshell and core, inserts and vertical rod) is 0.580 kg, according to the weight estimator in Hypermesh.
Within the support itself, a threaded aluminum insert is laminated, while two inserts with through-holes are laminated inside the mainplane to accommodate the screw heads. The two components are connected using four screws inserted and tightened from four holes on the suction side of the mainplane. Inside the mainplanethere are no guides for inserting and aligning the screws, containing only the foam core. Furthermore, the axes of the insert holes are perpendicular to the component surface and not aligned with the z-axis. Consequently, during the mounting process, it is common for the screw, in an attempt to align with the hole axis, to inadvertently enter the foam core, causing carving and damage. In some cases, the screw may become stuck in the foam core, resulting in a challenging assembly of the two components and poor ergonomics.

Figure 2. Rear Wing Supports 2022

2.2 Manufacturing

The 2021 rear wing was all made of an outer shell structure of carbon fibre with epoxy resin matrix and an inner core of a rigid foam.
Mainplane and supports are produced with T1100 prepreg, a high modulus carbon fibre, while Flaps Beam and Endplates were produced through wet layup with Textreme, a spread tow carbon fibre plain weave. Its properties are given by the producer, obtained after impregnating it with UTS50 fibre and Axiom 5206 epoxy resin.

T1100		
Tensile Elastic modulus 0° (90°)	[GPa]	84.5 (82.7)
Compressive Elastic modulus 0° (90°)	[GPa]	75.2 (77.4)
Tensile Strength 0° (90°)	[MPa]	1452 (1212)
Compressive Strength 0°(90°)	[MPa]	732 (702)
Density	[g/cm3]	1.53
Surface density	[g/m2]	200

Table 2. T1100 Carbon fibre properties

Textreme		
Tensile Elastic modulus 0° (90°)	[GPa]	64.6
Compressive Elastic modulus 0° (90°)	[GPa]	58.2
Tensile Strength 0° (90°)	[MPa]	1300
Compressive Strength 0°(90°)	[MPa]	650
Density	[g/cm3]	1.51
Surface density	[g/m2]	80

Table 3. Textreme Carbon fibre propperties

Pressure and suction surface shell were cured separately in their respective moulds. Subsequently, they were joined together in the Trailing Edge and Leading Edge regions. During this operation, the Rohacell core was also adhered to the carbon fibre structure, utilizing the moulds as a guide for precise alignment. The foam core was milled with a slight excess of material to ensure proper compression against the carbon fibre structure during assembly. The adhesive between the outer shell and inner core was applied at various points along the surface, resulting in non-continuous bonding between the two components.
Flaps and mainplane are mounted to the endplates through threaded inserts wrapped on the carbon fibre structure. The lateral faces of the elements are laminated onto two plates are screwed to each mould at its extremities.

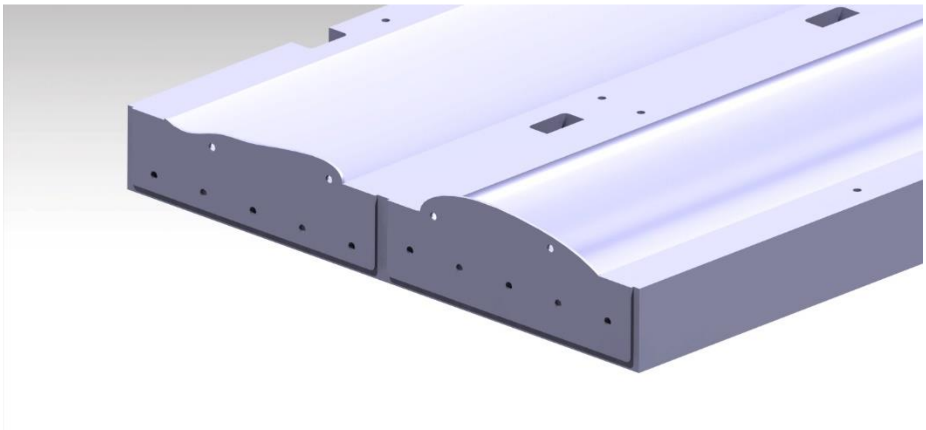

Figure 3. 2021 Flap mould

RW 2021				
Composite Shell	**Material**	**n° plies**	**Layup**	**Weight [kg]**
Main	T1100	3	0-45	0.474
Flap 1	Textreme	7	0-90	0.45
Flap 2	Textreme	3	0-90	0.22
Flap 3	Textreme	4	0-90	0.291
Support (single component)	T1100	10	0-45	0.44
Endplate (single component)	Textreme	2/side	0-45	0.343

Table 4. Rear Wing 2021 laminate configuration

RW 2021				
Core	**Material**	**Weight [kg]**	**Inserts**	**Weight [kg]**
Main	Rohacell IG 31F	0.439	CFRP & Ergal	0.0066
Flap 1	Rohacell IG 31F	0.037	CFRP	0.009
Flap 2	Rohacell IG 31F	0.072	CFRP	0.009
Flap 3	Rohacell IG 31F	0.049	CFRP	0.009
Support (single component)	Rohacell IG 31F	0.035	CFRP & Ergal	0.0034
Endplate (single component)	Rohacell IG 31F	0.079	CFRP	0.0057

Table 5. Rear Wing 2021 core configuration

Total	Estimated weight [kg]	Real Weight [kg]	Difference %
Main	0.913	1.555	70.3
Flap 1	0.487	0.424	-12.9
Flap 2	0.292	0.388	32.9
Flap 3	0.34	0.387	13.8
Support Left	0.475	0.55	15.8
Support Right	0.475	0.531	11.8
Endplate left	0.422	0.722	71.1
Endplate Right	0.422	0.661	56.6
Total	3.878	5.218	34.6

Table 6. Rear Wing 2021 estimated and real weight comparison

The variance between the estimated weight and the actual weight can be attributed to several factors. In the case of the mainplane, which exhibits the largest difference, the higher weight is primarily a result of the glue used to bond the core material with the outer shell. This adhesive was not factored into the Hypermesh weight estimation and has a significant impact due to the substantial surface area of the component. Additionally, the glossy finish and applied paint for aesthetic purposes contribute to the increased weight.
For the flaps, which are produced through a wet layup process involving manual resin application by team members, the weight discrepancy arises from the non-uniform quality of manufacturing. The team's limited control over the resin application to the carbon fiber plies impacts the overall weight. This effect is more noticeable in the endplates, where not only is the actual weight higher than the estimated weight, but there's also a weight difference between the left and right endplates due to the inherent non-repeatability of the manual manufacturing process.

2.3 Structural analysis results of Rear Wing 2021

Simulations performed in 2021 only accounted for aerodynamic load, since showed to be the most severe one. The aerodynamic forces were modelled through RBE3 for each wing element, with the dependent node located in the centre of pressure, while the independent nodes are the ones of the pressure surface. The drag and downforce are applied to the centre of pressure. This method is though incorrect since it does not replicate correctly the way in which the aerodynamic load act on the components.
A summary of the aerodynamic forces is shown below.

	2021	
	Downforce [N]	**Drag [N]**
Main	315	9
Flap 1	126	43
Flap 2	136	111
Flap 3	57	95
Beam	/	/
Total	634	258

Table 7. Rear Wing Aerodynamic forces

By looking at the support composite stresses, is evident that the component is working in a inefficient way. The maximum stress is of 35 MPa, located in the area around the screw holes, while the rest of the component has stresses around 15-20 MPa and other areas with null stress, having so a part of the component that is not working at all with the consequence of just adding weight to the structure. It must be pointed out that low stresses are a consequence of the high stiffness required for the supports, to minimize the deflections under the aerodynamics load and during the technical inspections. It is anyway evident that the support geometry can be optimized for the structural purpose and so to reduce its weight.

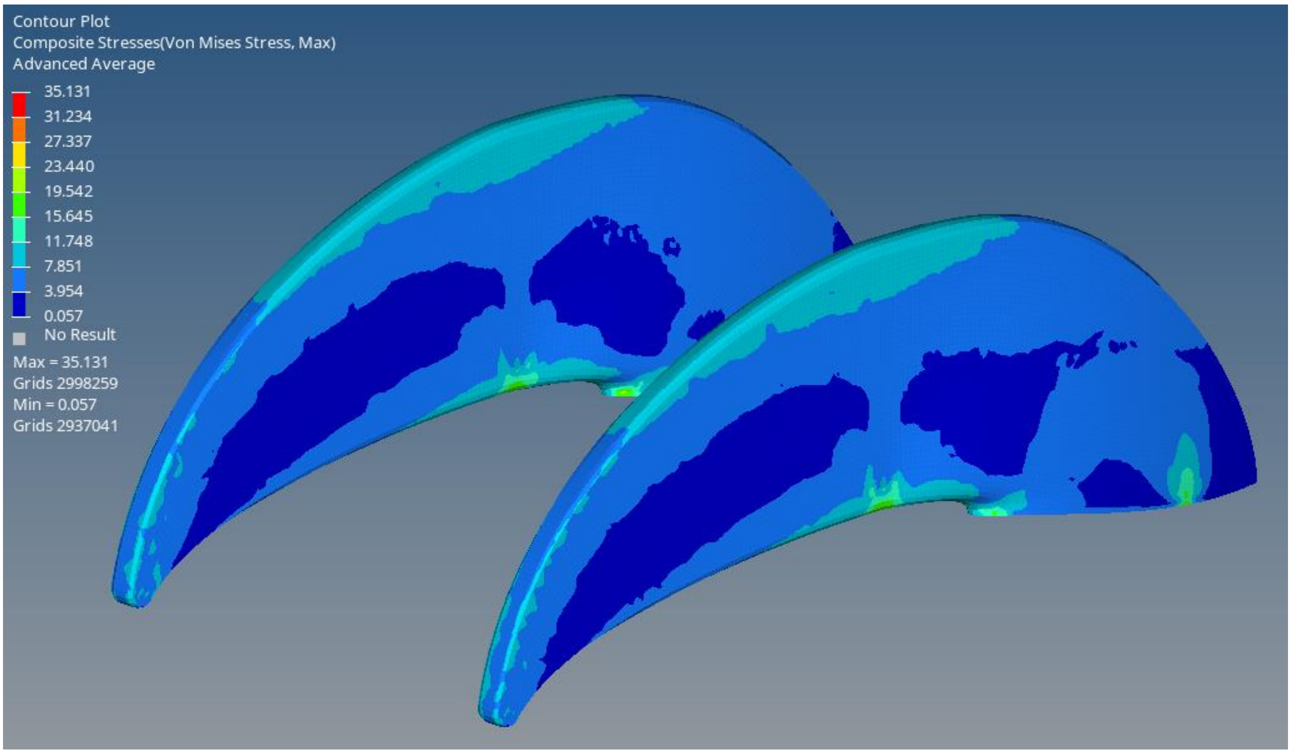

Figure 4. Support 2021 - Composite Stress

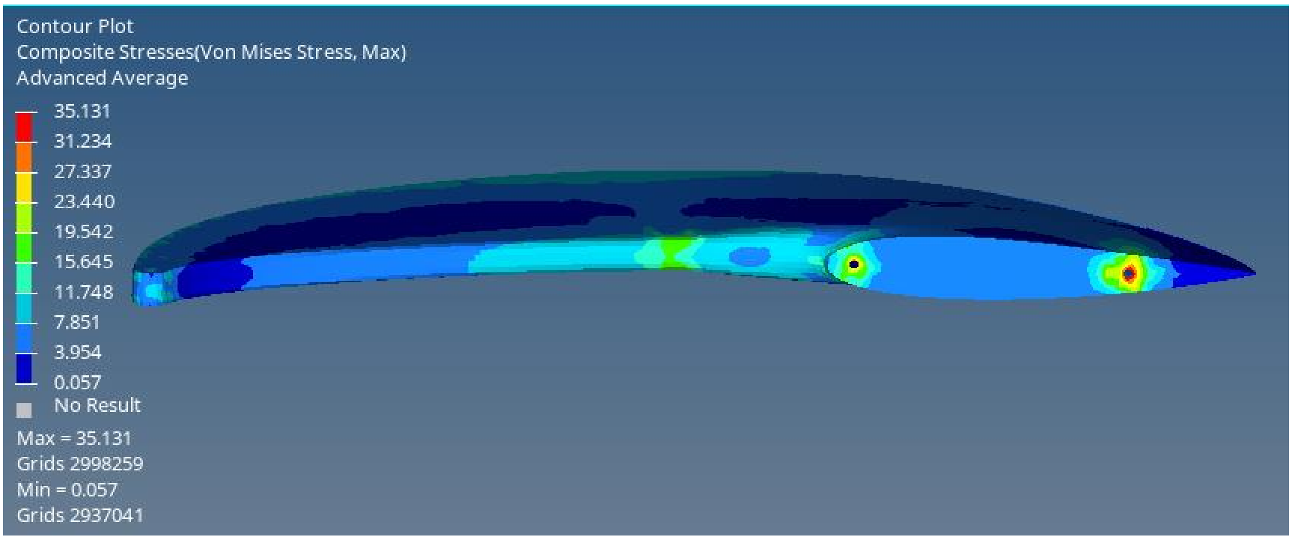

Figure 5. Support 2021 (screw holes) - Composite stresses

Same trend can be observed in the main and the flaps, where generally low stress are encountered in the structure, but here as well the low stresses are a consequence of the high stiffness needed.

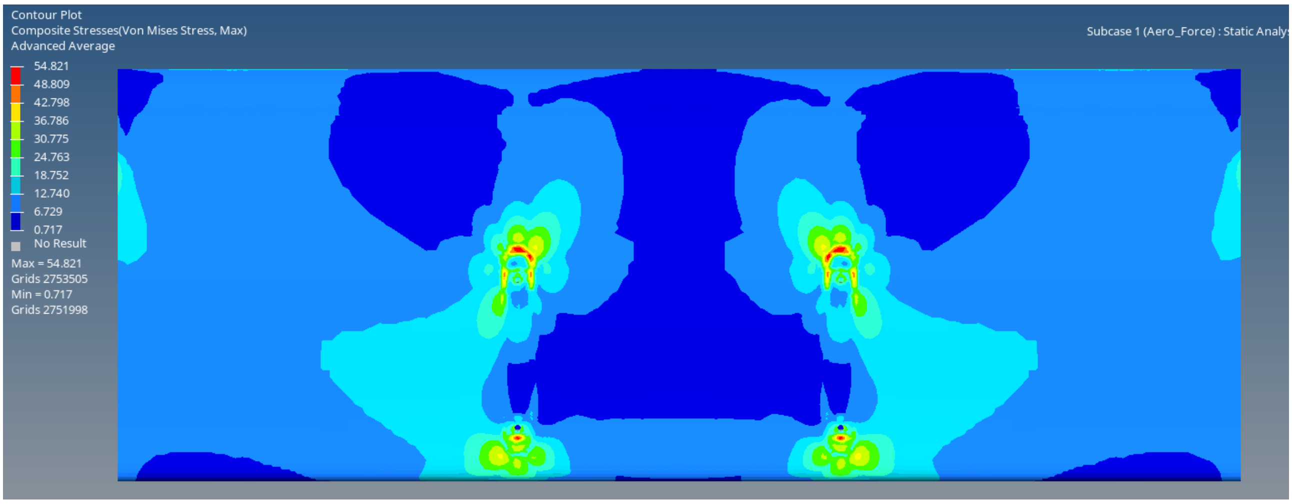

Figure 6. Mainplane 2021 (pressure side) - Composite Stress

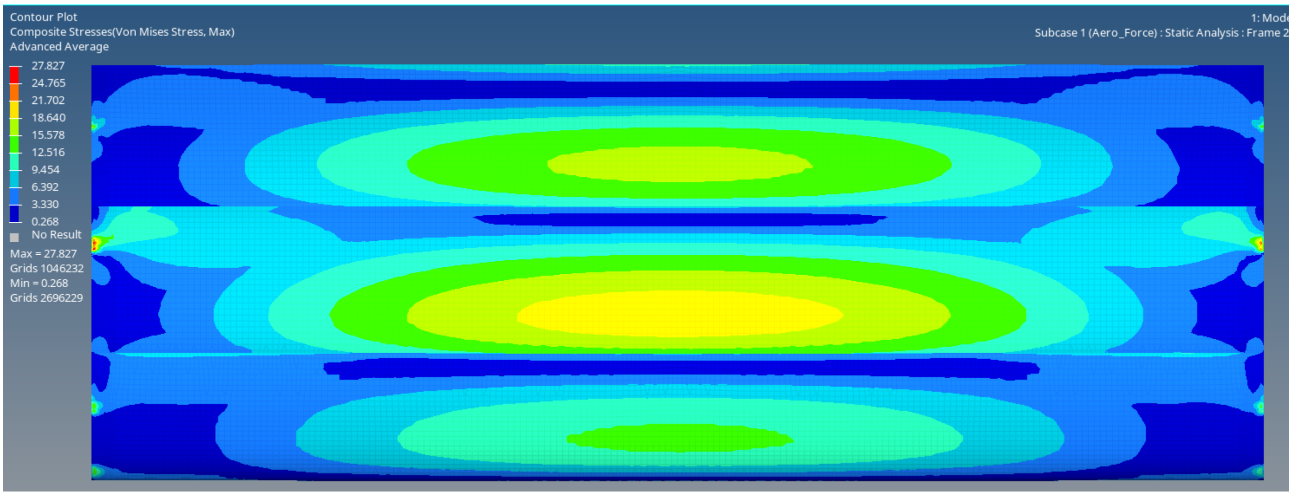

Figure 7. Flaps 2021 (suction side) – Composite Stress

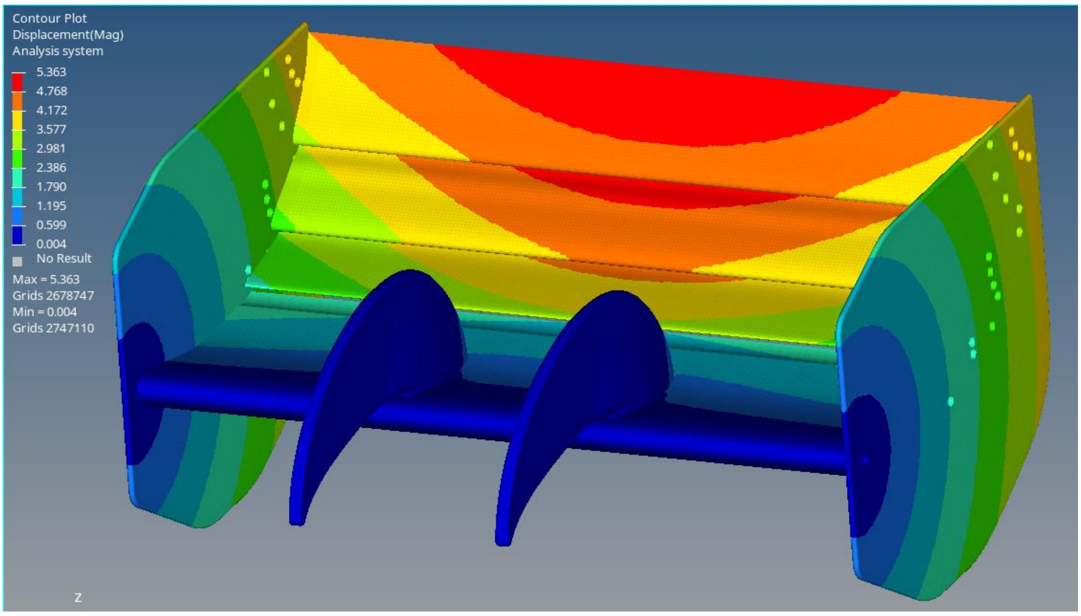

Figure 8. Rear Wing 2021 - Displacement

2.4 Mainplane failure

During a test session in the 2022 season, it was registered a failure in the Mainplane of the rear wing.
A deep analysis of the component was not done since it was a one-off that must be used for the race of that season, so it was fixed by injecting epoxy resin through some holes in the pressure side of the component. Thus, it was not clear what happened to the component.
The main hypothesis for the reason of the failure was that there was an excessive offset from the wing support's to the centre of pressure of the wing.
This would result in an excessive arm of the bending moment that caused excessive stress in the component, causing its failure. To confirm this hypothesis, a simulation of the component with a backward positioning of the wing support was performed, confirming that the excessive offset results in higher stress in the component. Simulation was performed with the aerodynamic forces acting on the moment of the failure, therefore the aerodynamic force of 2022 Rear Wing.
Another factor that can have an influence on the failure of the component is that in 2022 was added the beam element to enhance the performances of the wing, increasing the aerodynamic forces to which the component was subjected.

	RW 2021		RW 2022	
	Downforce [N]	**Drag [N]**	**Downforce [N]**	**Drag [N]**
Main	315	9	396.48	22.49
Flap 1	126	43	151.7	61.32
Flap 2	136	111	139.02	132.44
Flap 3	57	95	62.28	102.5
Beam	/	/	92.2	31.48
Total	634	258	841.68	350.23
Difference	/	/	**+32.76%**	**+35.75%**

Table 8. Aerodynamic forces comparison

The image below depicts a comparison between the 2021 mainplane (on the left) and the version with backward positioning of support attachment (on the right). Simulation results reveal a notable reduction in maximum stress on the carbon fiber shell, decreasing from 27 MPa to 16 MPa by moving the supports backward by 80mm. This results in a substantial 41% decrease in maximum stress.
Regarding the core, it is evident that the maximum compressive stress on the material reaches 0.307 MPa, particularly in the area just behind the rear attachment point of the support, which is very close to the ultimate compressive strength of the material at 0.4 MPa. Consequently, due to the car encountering road irregularities and bumps, the actual stresses surpass the simulated values, leading to a failure in the component in that specific area. Team members present during the event observed and reported this failure.

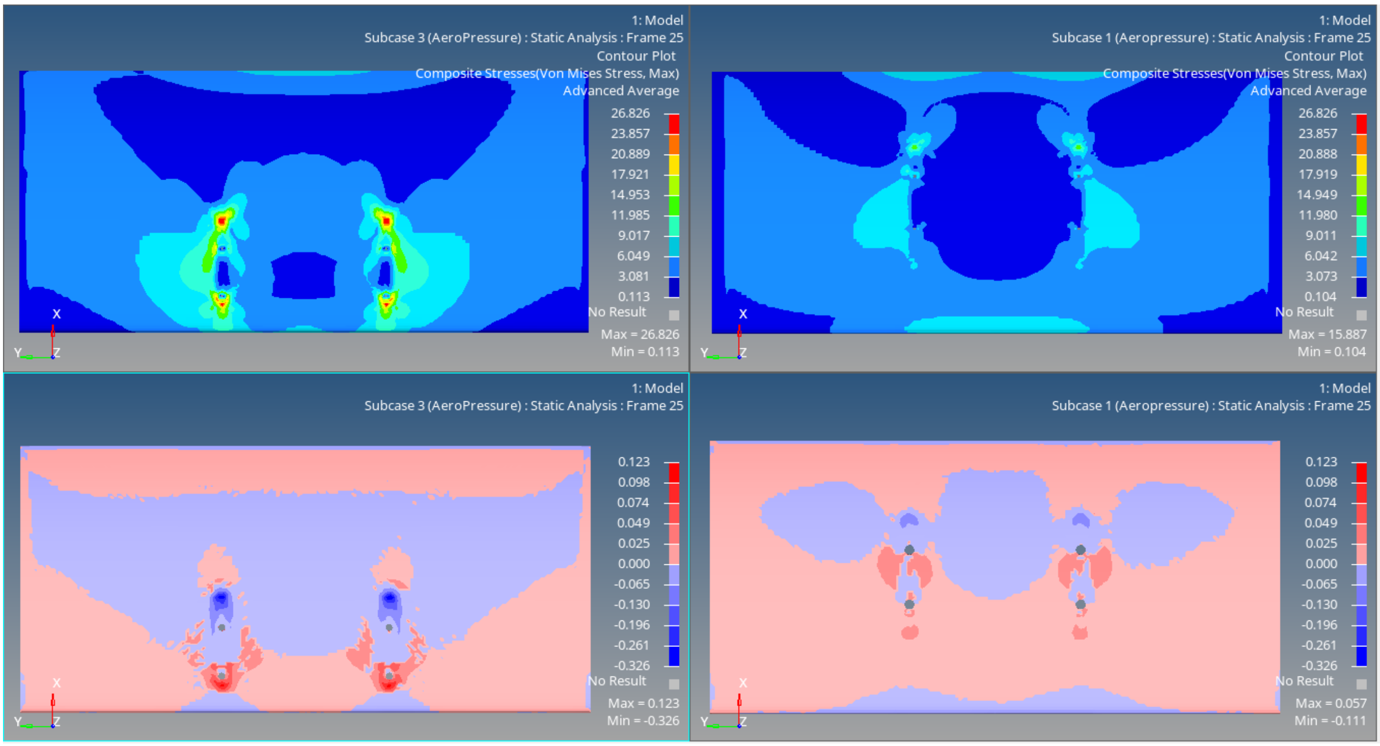

Figure 9. Mainplane - Composite Stress (up); Core Stress (down)

3. Design of Rear Wing 2024

This chapter is devoted to shaping the design of the Rear Wing for the upcoming season, leveraging insights gained from the detailed analysis in the previous chapter.

3.1 Introduction

Over the past three seasons, the team's aerodynamic components were crafted from a carbon fibre shell with epoxy resin and an inner core of machined rigid foam. While this approach was validated by the team's experience, it proved to be relatively expensive due to the core material cost and the milling process needed for the final shape. To address this, the team leverages the thermoforming capability of Rohacell and the sufficient flexibility of low-thickness Nomex Honeycomb panel, producing hollow wing elements with sandwich-structured shells to resist shear loads. This innovation reduces material usage and eliminates the milling process, resulting in significant time and cost savings.

The first item to be repurposed from the team's existing equipment is the moulds from the 2021 components. These moulds will be milled again for the new wing geometries, with the flaps mould made of WB-0700—an epoxy board known for high-temperature resistance and suitability for carbon fibre lamination due to low thermal expansion. The mainplane mould is crafted from aluminum, that solves the problem for pressure and temperature but must be accounted its thermal dilatation for the curing process.

Thales Alenia Space sponsors the high modulus 5HS prepreg carbon fibre used for the components, while FTS SpA provides 220gsm twill carbon fibre cloth, the properties of which were determined through traction tests. Recycled fibre Rymyc cloth with resin infusion is used for inserts.

The prepreg carbon fibre requires curing at 150°C and 6 bars for 3 hours, making it unsuitable for the flaps due to the WB 0700's maximum temperature tolerance of 130°C. Consequently, flaps and beamwing components are manufactured using wet layup with the FTS fabric. The prepreg is reserved for producing supports, laminated on a flat steel panel, and for the mainplane, utilizing available aluminium moulds.

An alternative method considered involved creating a carbon fibre mould through resin infusion with the 220gsm carbon fiber provided by FTS, along with Rymyc fiber to increase wall thickness, on the WB 0700 mold. The prepreg would then be laminated onto the carbon fiber mold. While this approach could yield higher-quality cured components with matched thermal expansion coefficients between mould and component, its complexity and resource requirements led to the decision for a more easily controllable process.

All composite material components are manufactured in-house by team members who lack specialization and have limited experience in this field. This necessitates a conservative design approach for the entire wing assembly to mitigate the risk of unexpected failures due to non-conformity between design specifications and actual production capabilities.

Based on the CFD simulation conducted at a speed of 60 km/h, which corresponds to the design speed of the aerodynamic assembly, it was observed that the aerodynamic package maintains stable aerodynamic performance with a maximum displacement of up to 5mm. Even though, the optimal maximum displacement is of 2.0 mm for the components at a vehicle speed of 60 km/h. This target also accounts for any approximations introduced in the

numerical model used for the structural analysis, because final displacements in real components will results higher than the numerical estimated ones.
In the following paragraphs, the parts constituting the Rear Wing assembly and the chosen manufacturing processes for their production will be presented.

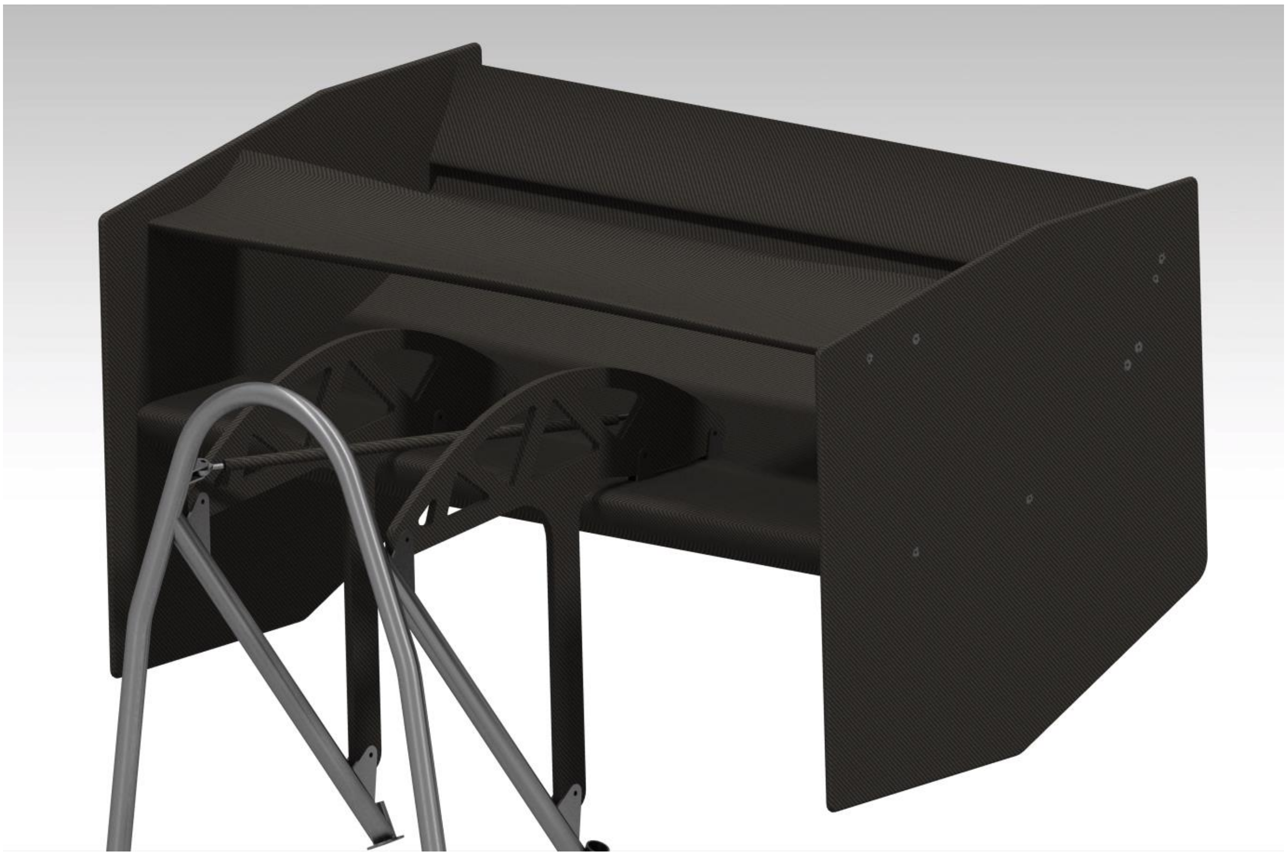

Figure 10. Rear Wing 2024

3.2 Wing Assembly Components

3.2.1 Supports

The starting point for the design of the 2024 Rear wing is the supports assembly. The design of the support starts from its attaching point to the Main Hoop structure and the location of the mainplane anchoring point. The upper side is rounded to create less turbulence that would affect the aerodynamics of the wing.
As was seen in support of 2021 assembly, the central area of the part (from side view) is not effectively working. The same trend can be observed in the 2024 version, therefore were practiced some opening, triangulating the structure, to eliminate material in the area where is not properly needed, decreasing its weight by 24%.

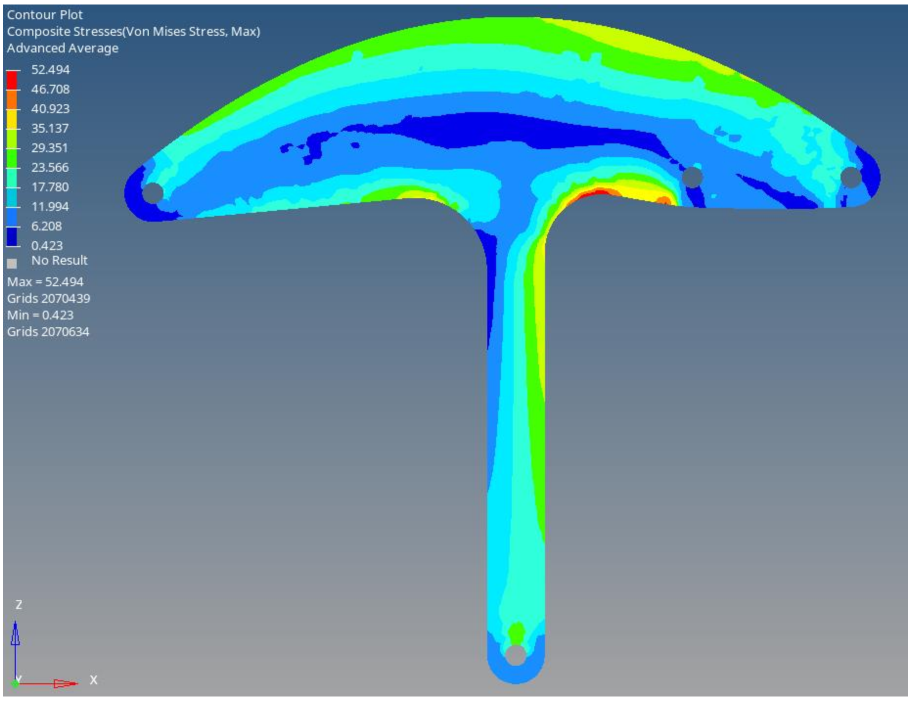

Figure 11. Support composite stress without lightening cut

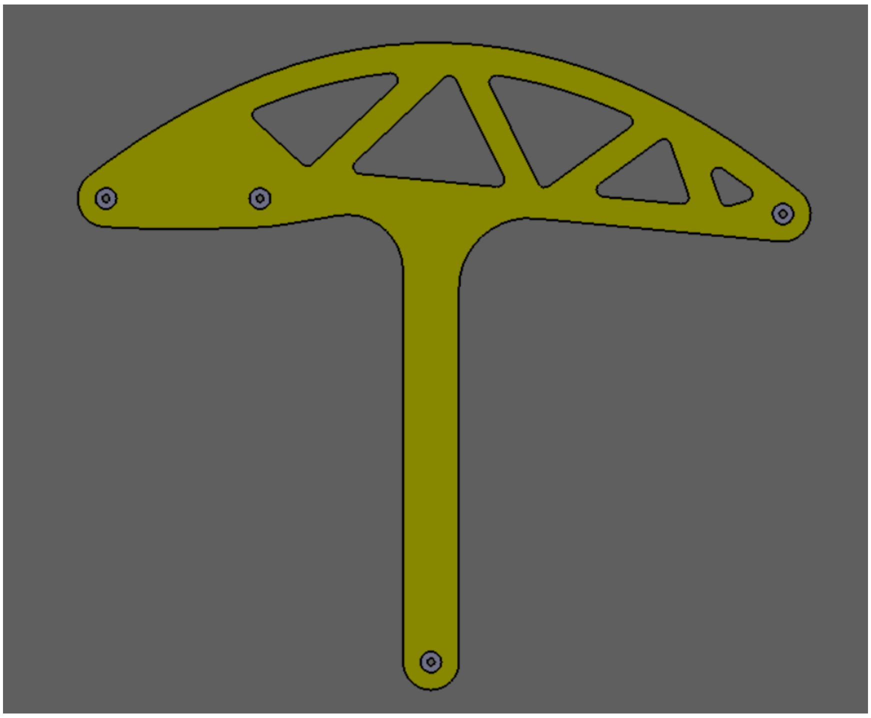

Figure 12. Support 2024 geometry side view

They are attached to the vehicle structure on the two nodes of the bracing and on the upper point of the Main Hoop for the diagonal rod, needed to triangulate the structure for the lateral loads. Moreover, with this geometry is not anymore needed the vertical pushrod to connect the support to the lower attachment to the main hoop since this function is performed by the component itself.

The supports are mounted to the mainplane through two ribs with 4 flanges each, where the support slide in, and fixed with two calibrated bolts. This largely simplify the mounting and dismounting process of the wing from the car compared to its previous version, where bolts where inserted from the two holes on the suction surface of the mainplane.

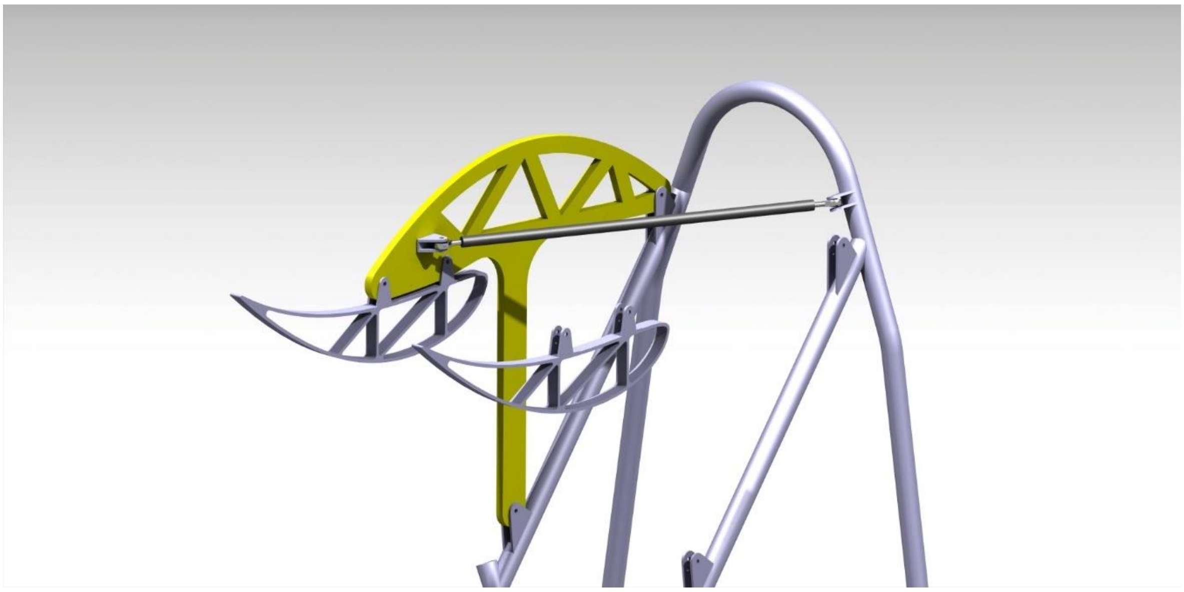

Figure 13. Support 2024 Mounting Structure

Supports are made by a sandwich structure composed of high modulus carbon fibre and a 10mm thick honeycomb panel with inserts wrapped on the carbon fibre structure. They are laminated between two flat steel panels - so no moulds are needed – with the borders of the panel covered by L shaped profile to prevent the vacuum bag pushing against the honeycomb and causing its crash. Panel is cut with waterjet after the curing process, allowing to obtain complex shape without requiring complex production methods. A single carbon fibre ply is then wrapped with wet layup around the border of the supports to cover the exposed honeycomb.

3.2.2 Mainplane

The mainplane is a hollow component, made with Thales Alenia prepreg and a sandwich structure a 2 mm honeycomb panel as core material. To avoid crash of the core material, since it is wrapped by the carbon fibre ply and so the pressure is acting against lateral face of the panel, is needed to make a chamfer on the edges of the honeycomb sheet of about 30 degrees from the horizontal.

Figure 14. Honeycomb panel with edge chamfer to avoid crash during curing process

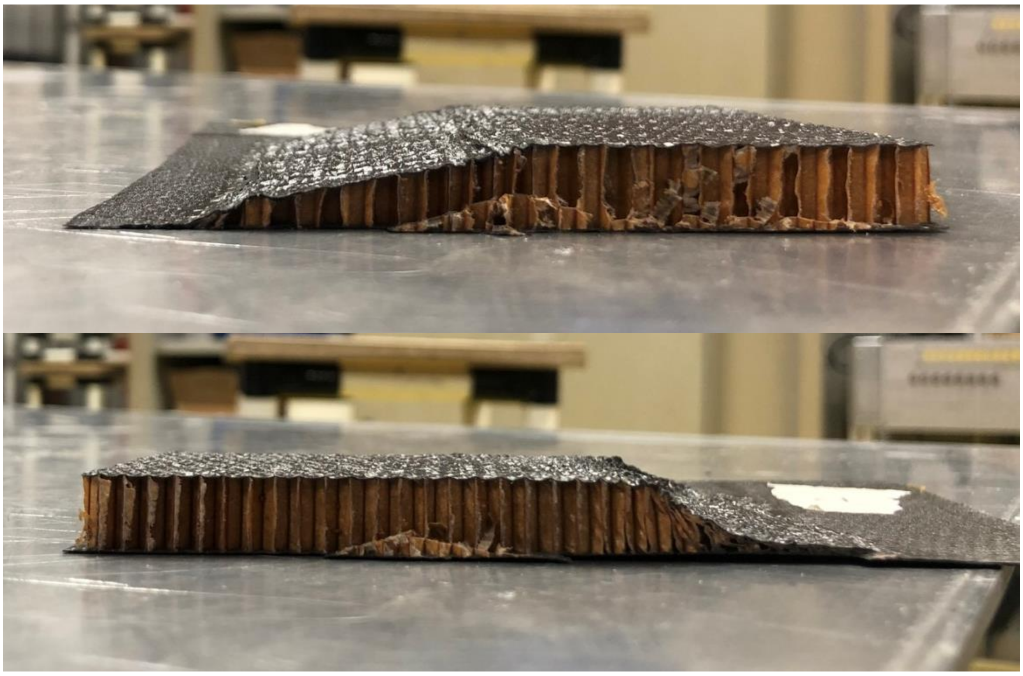

Figure 15. Cured sandwich panel with different edges chamfer angle

The sandwich structure does not cover the whole surface, but it has a margin of 1 cm from the trailing edge because of lack of space and 2 cm from the leading edge because of the high curvature of the surface in that area.
The pressure and suction surface are laminated as two separate shells that are then glued together on the trailing edge and the leading edge. To improve the gluing surface, in the trailing edge the plies have a small excess that is folded on itself – helping as well to strengthen the section in that point – that creates a thicker border that increase the contact area. In the leading edge, instead, is used an extra mould on top of the suction side mould to extend the laminate for 1cm further from the edge, so that the shells are glued not only along the border but also on this additional surface, as can be seen in the sketch below.

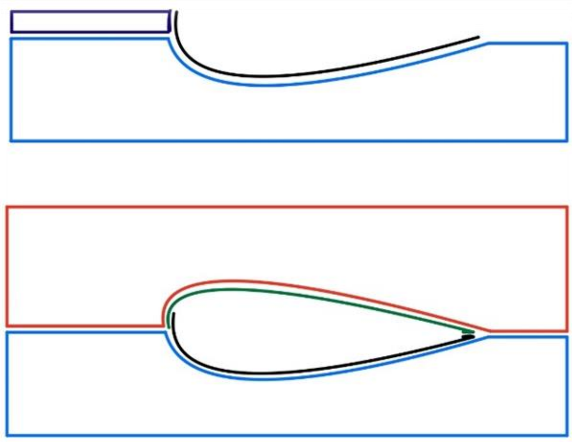

Figure 16. Mainplane shells gluing method

Inside the mainplane are placed four ribs: two at the extremities to be mounted on the endplates; two in the central area to mount the supports.
As for the 2021 Rear wing, the centre of pressure of the aerodynamic forces is backwards the position of the supports, so this generate a bending moment for the structure that can be critical if not balanced. A solution for this could be moving the supports attachment point backwards along the mainplane chord, but this would result in an excessive disturbance to the airflow, creating separation of the air from the mainplane surface, thus compromising the aerodynamic performances. So was decided to place two ribs in correspondence of the supports to strengthen the structure while keeping the supports close to the leading edge.

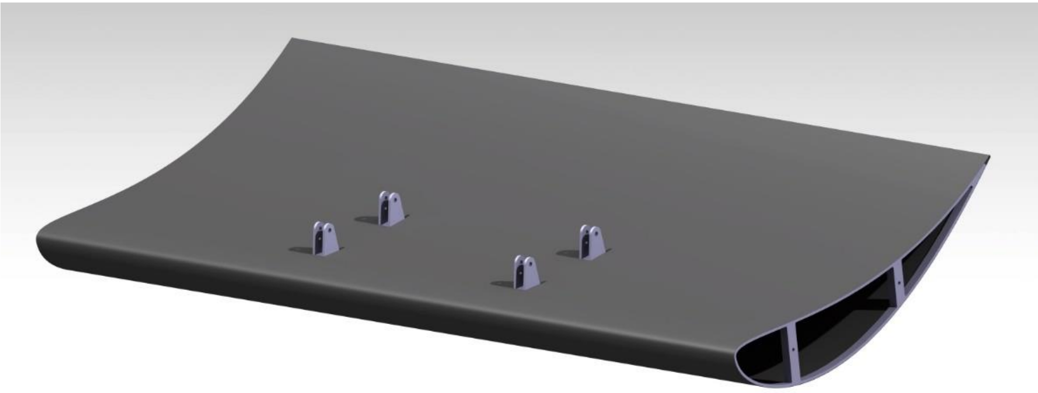

Figure 17. Mainplane assembly

3.2.3 Flaps and Beamwing

Flaps and Beamwing, as well as mainplane, are hollow components made of a sandwich structure with 2mm Rohacell IG-31 F as a core, with the difference that, compared to the mainplane, the pressure and suction surface are a single piece. To do that, the two shells are laminated on their respective moulds, but the plies have, in the leading edge, an offset one from the other so that, when the mould are coupled to join the shells, there is an overlap between the plies, as shown in the sketch below. Resin infusion technique is chosen for these components, that is possible thanks to the closed-cell structure of the Rohacell IG, so that the panel do not absorb the resin during the process.
The two flaps share the same geometry, therefore a single mould for pressure and suction side is needed. The end ribs as well are equal between right and left side, so the same component can be used for all four extremities of the flaps.

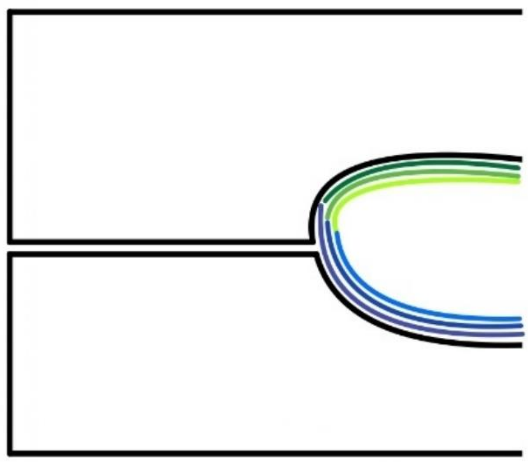

Figure 18. Plies overlap in the leading edge

Before closing the moulds together, a tubular vacuum bag is placed in the flap cavity, so it could be connected to the external bag that envelopes the entire moulds assembly to pull vacuum that pushes the carbon fibre structure to the moulds.
Ribs are glued to the structure after the curing process with Loctite EA 9466.

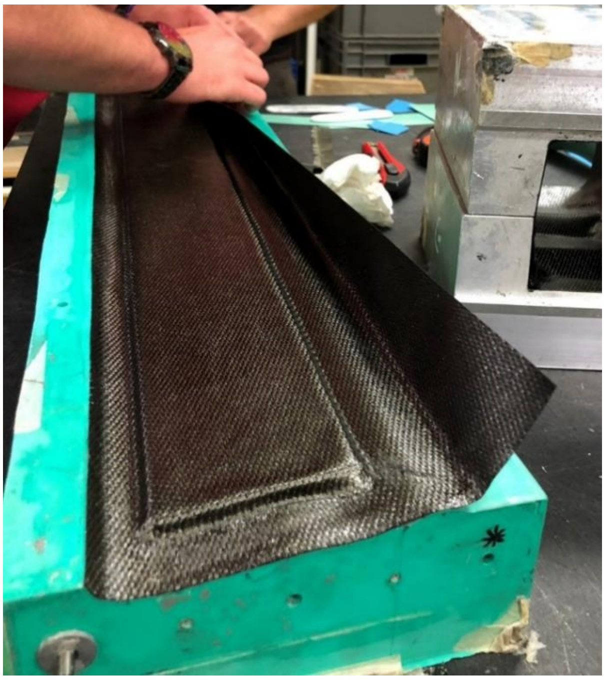

Figure 19. Flap sandwich structure and ply folding on trailing edge

Figure 20. Vacuum bag system with internal tubular bag

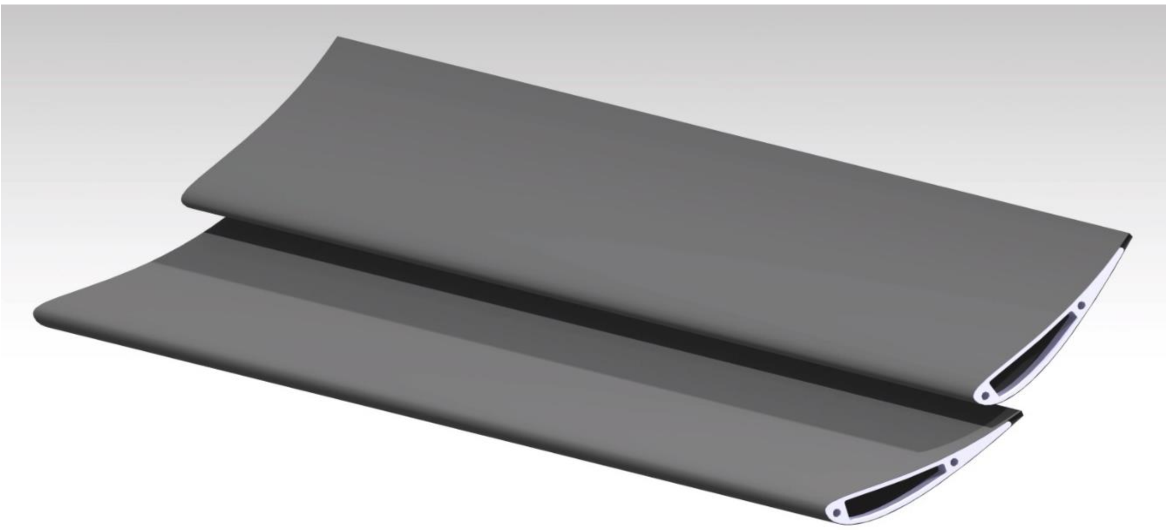

Figure 21. Flaps assembly

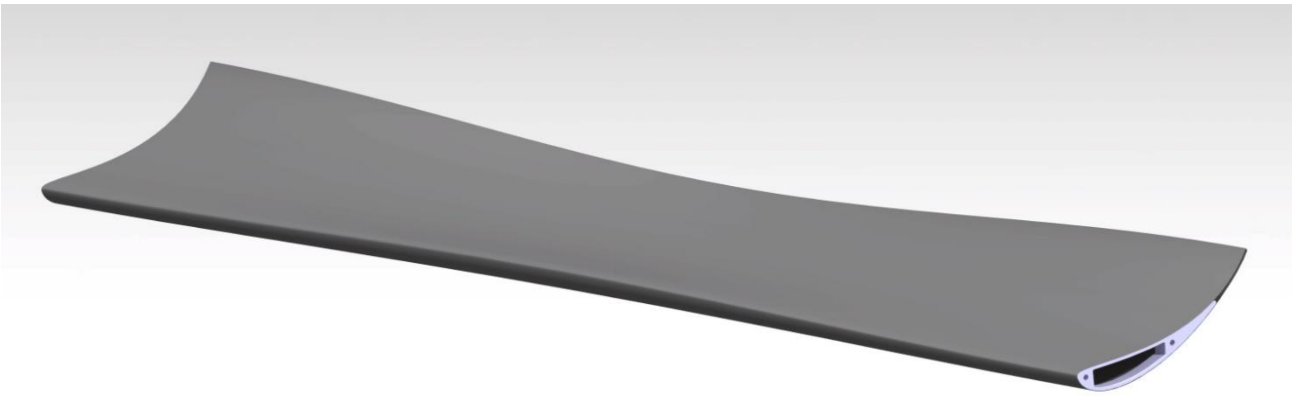

Figure 22. Beamwing assembly

3.2.4 Endplates

Endplates are a sandwich panel made with Thales Alenia prepreg and a 10mm thick honeycomb panel. The production method is the same one described for the supports. For the holes to mount the wing elements are used CFRP (carbon fibre reinforced polymer) inserts with through-holes made of Rymyc recycled fibres to resist against the screw tightening force.

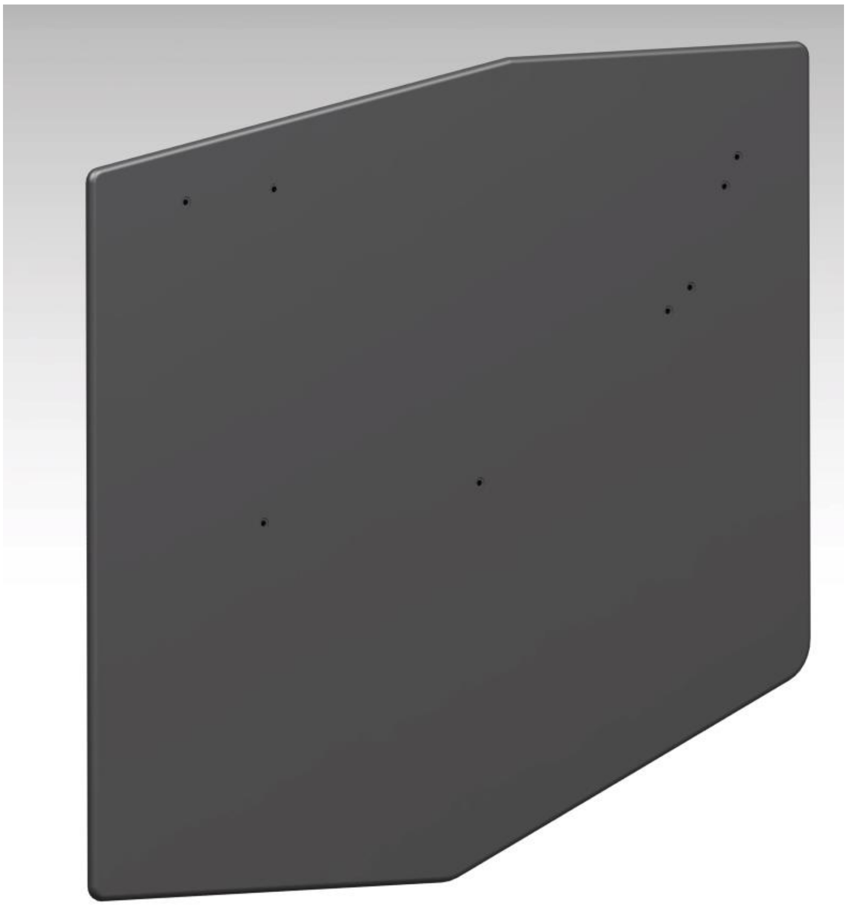

Figure 23. Endplate

3.2.5 Ribs

Ribs are used at the extremities of the wing element to have a solid structure and to allow the endplates to be mounted on the elements. They are made of Aluminium 6060 T6 since they are components subjected to low stresses. Thanks to the small load acting on end ribs, is not necessary to triangulate their geometry, allowing to have only one central opening on the cross section, a necessary feature to produce flaps and beamwing with internal tubular vacuum bagging film. All the extremity ribs are obtained from a 10 mm thick plate and cut with waterjet. The end ribs are identical for the same elements, therefore for the flaps the same rib is used in the four extremities. Different geometries are used for the beamwing and the mainplane.

The central ribs of the mainplane, differently from the extremity ones, are entirely machined because would not be possible obtaining them from only waterjet cut. Even in this case, the two ribs are the same.

Figure 24. Flaps end rib

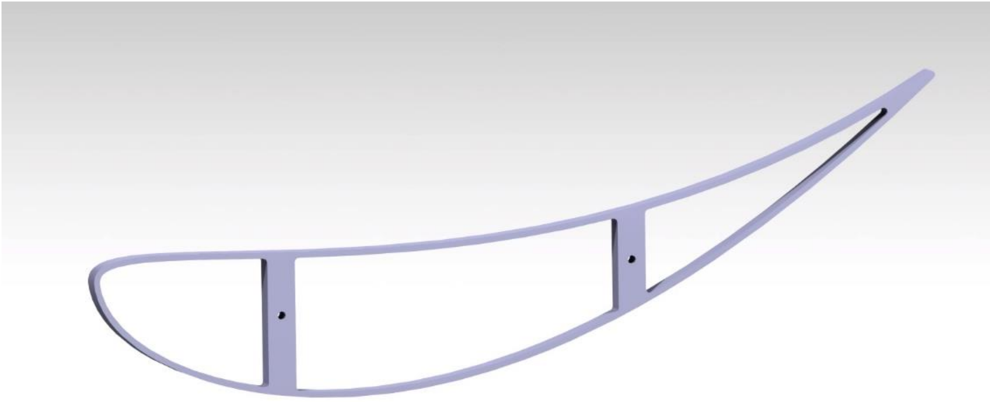

Figure 25. Mainplane end rib

Figure 26. Mainplane central rib

3.2.6 Rod

The only rod in the wing assembly is used to connect the left support to the main hoop to triangulate the structure in the XY-plane. Rod is made of carbon fibre with 90% of unidirectional plies and an external layer of twill fabric.It is connected to the mainhoop through two welded flanged and to the support through a glued flange on the lateral surface.

Figure 27. Diagonal Rod for triangulating support structure

3.2.7 Inserts

Inserts are employed only in endplates and supports and are made by Rymyc, a cloth of recycled short carbon fibre, with resin infusion technique and then cut with waterjet. The plies are used to realize a slab through resin infusion technique and subsequently it is cut with waterjet to obtain the necessary shapes. Thanks to the easiness with which can be produced and their mechanical performance, Rymyc inserts can substitute the aluminium inserts, when through holes are needed since carbon fibre cannot be threaded, with the advantage of easy production and lighter weight.
For endplates and supports are used cylindrical-shaped inserts, as the one that can be seen in the picture below, in correspondence of the screw holes and they are wrapped to the carbon fibre structure.

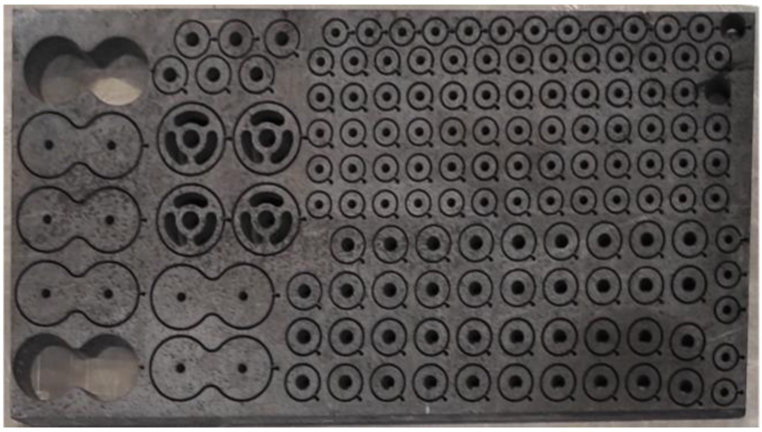

Figure 28. Rymyc inserts slab

3.3 FEM modelling

For the FEM analysis was used Altair Hypermesh with Optistruct solver. The structure simulated includes only the supports assembly and the wing assembly. The mainhoop was not included in the analysis and it is supposed to be infinitely rigid compared to the other components since its made of steel, so its stiffness is about three times larger than the component of the wing assembly. In this way the constraints are applied to the supports in the attachment point to the main hoop, allowing to have a less complex model and save computational time.

For the wing elements, the endplates and the supports, who are all made of composite material, the property assigned to the components has the card image PCOMPP since they are all modelled with ply-based composite definition. Two different properties for the composite materials are used because some are modelled with an extracted midsurface, that works as the middle plane of the laminate, while other are modelled with their external surface, so the laminate is created extruding from that surface towards the inside of the component.
A summary of the components of the assembly, the properties used to model them and the materials used, with their respective properties, are shown in the tables below. It follows then a more detailed description of their modelling in the Hypermesh software.
The mechanical properties of the Rymyc inserts are obtained by previous studies made by the team through compression test. Due to the not uniform spread of the resin among the several plies, the weight of the insert is not constant. The density value used for the weight estimation in Hypermesh is an average of the densities measured from the several inserts.
The mechanical properties of the carbon fibre used or the wing components were obtained from traction test that will be described later.

Component	**1D/2D/3D**	**Property Card Image**	**Material**
Wing elements	2D	PCOMPP (z0: Bottom)	220gsm Twill Carbon Fibre – Rohacell IG 31F
Supports	2D	PCOMPP (z0: Real)	160gsm 5HS Carbon Fibre prepreg – Nomex HRH10-3.2-48
Endplates	2D	PCOMPP (z0: Real)	160gsm 5HS Carbon Fibre prepreg – Nomex HRH10-3.2-48
End Ribs	3D	PSOLID	Al 6060 T6
Support Ribs	3D	PSOLID	Al 6060 T6
Inserts	3D	PSOLID	Rymyc fibre
Bolts	1D	PBEAML	Steel 8.8 Class
Rod	1D	PROD	ItalTubes S type Carbon Fibre

Table 9. Wing Assembly components modelling

Composite Material	**Elastic Modulus [GPa]**	**Tensile Strength [MPa]**	**Ply Thickness [mm]**	**Density [g/cm3]**
160gsm 5HS Thales Alenia	103.23	504.15	0.14	1.26
220gsm Twill FTS	45.59	496.5	0.28	1.43

Table 10. Carbon fibre/epoxy resin composite material mechanical properties

Core Material	**Compression**		
	Elastic Modulus [MPa]	**Strength [MPa]**	**Density [g/cm3]**
Nomex HRH-10-3.2-48	138	2.24	0.048
Rohacell IG 31 F	17	0.4	0.031

Table 11. Core materials mechanical properties

Aluminium Alloy	Elastic Modulus [GPa]	Yield Strength [MPa]	Density [g/cm3]
Al 6060 T6	69	150	2.7

Table 12. Aluminium alloy mechanical properties

Rymyc Inserts	Compression		Density [g/cm3]
	Elastic modulus [GPa]	Strength [MPa]	
In-plane direction	3.16	125	1.6
Out-of-plane direction	1.81	200	

Table 13. Rymyc inserts mechanical properties

Rod	Elastic modulus [GPa]	Tensile strength [MPa]	Density [g/cm3]
Italtubes S series	115	2900	1.52

Table 14.carbon fibre rod mechanical properties

3.3.1 Components

Supports and Endplates

Supports and Endplates are modelled with midsurface, extracted from the original geometry, thanks to their symmetric shape. Differently from the wing elements, a specific property was defined for these components because of the definition needed for the z0 value of the laminate. In this case, since the midsurface lay in the centre of the component, the laminate is defined as symmetric with respect to the extracted surface, therefore the z0 option is set as *Real*.

The geometry was refined on Hypermesh to get a better meshing of the component with a more regular pattern of elements. To better catch the stress gradient around the holes are used the washer split to create a spiderweb mesh. For the support was used a geometry with no fillets in the edges of the triangular holes to simplify the meshing process, because the fillets have small influence in the simulation results of the component.

For the supports is used Nomex Honeycomb HRH-10-3.2-48 with 10mm thickness for the core and Thales Alenia's carbon fibre prepreg for the outer structure.

In the endplates is used an 8mm Rohacell IG 31 F panel and the 220gsm FTS carbon fibre fabric.

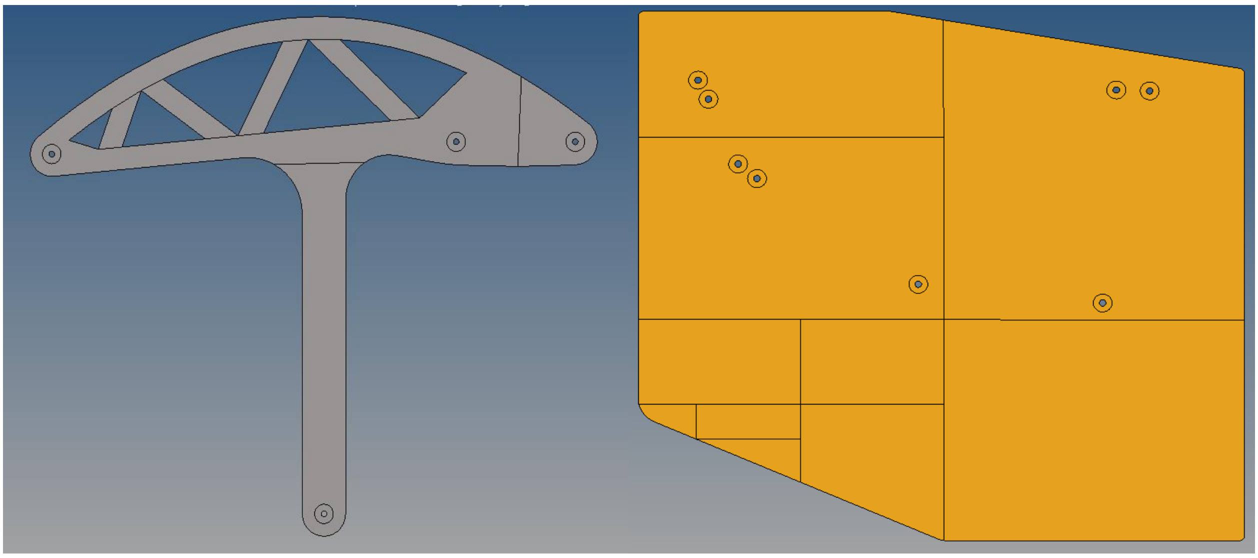

Figure 29. Geometry refinement for supports and endplate

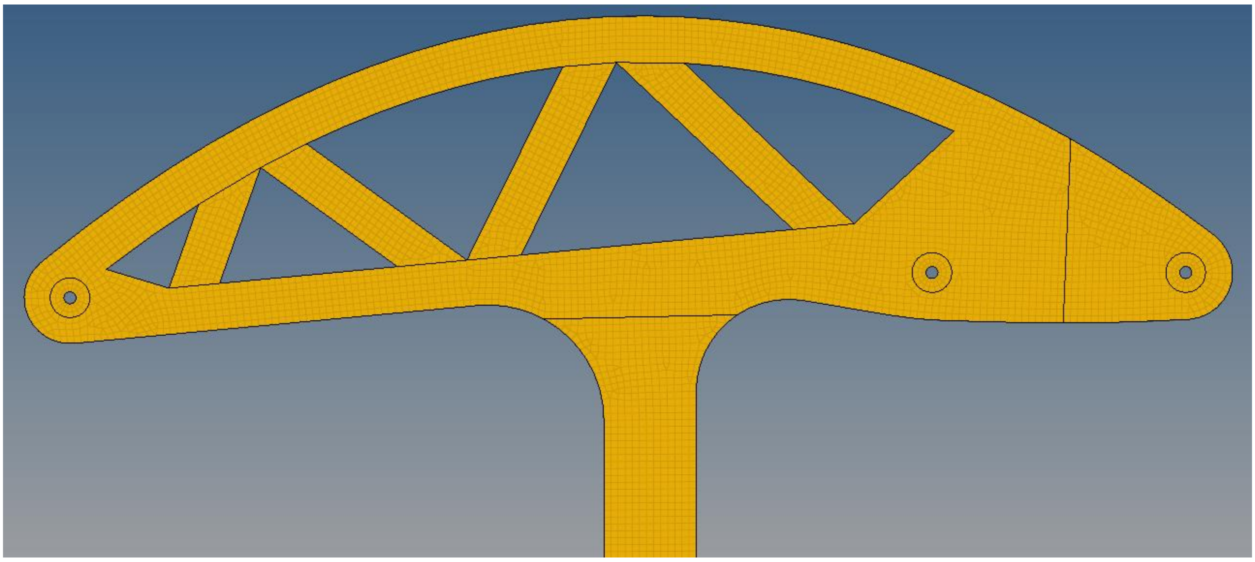

Figure 30. Support midsurface mesh

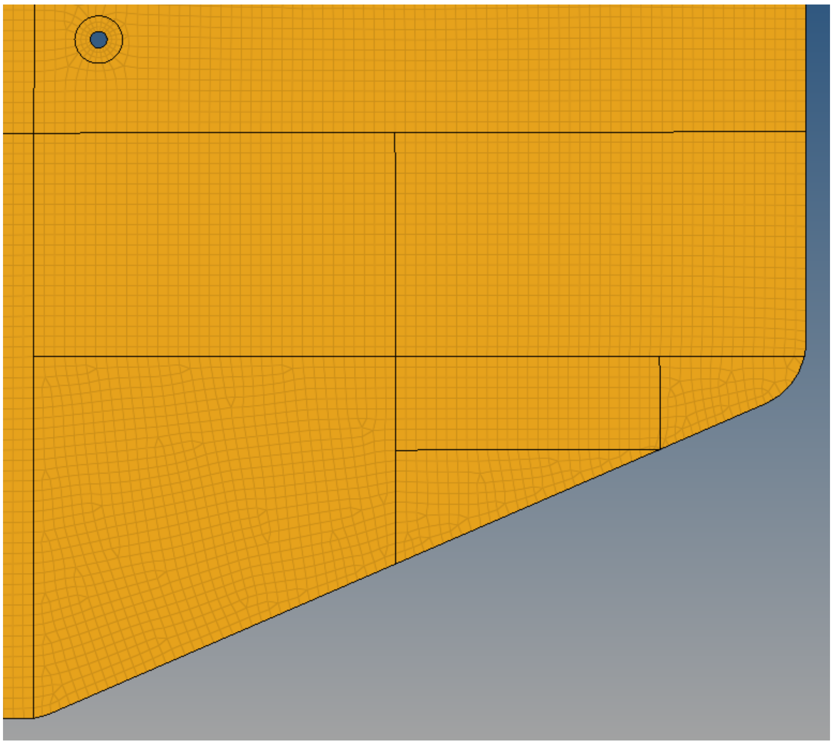

Figure 31. Endplate midsurface mesh

Mainplane, Flaps, Beamwing

For the flaps, beam and the mainplane, a mesh with only quad elements was done to obtain a regular and uniform mesh of the components. The normal of the elements is oriented inside of the component, while the fibre direction is aligned with x axis.
For those components was used another property, with respect to the Supports and Endplates that are modelled through Midsurface, since their normal and the reference surface for the laminate creation are oriented differently. Mainplane surface is modelled with the holes for the rib flanges to account for the stress concentration in that area. A geometry without holes is used for a simulation where the pressure map imported from the CFD solver was used, because otherwise it would create problems with the resultant of the aerodynamic forces in that component.
Property defined for those elements has card image PCOMPP with a z0 value defined as "BOTTOM", meaning that, according to the element normal definition, the surface of the model

represents the outer surface of the laminate, with the laminate that increases the thickness inwards the component.
The material used for the component is the 220gsm Twill carbon fibre from FTS with epoxy resin, whose property where already reported before.

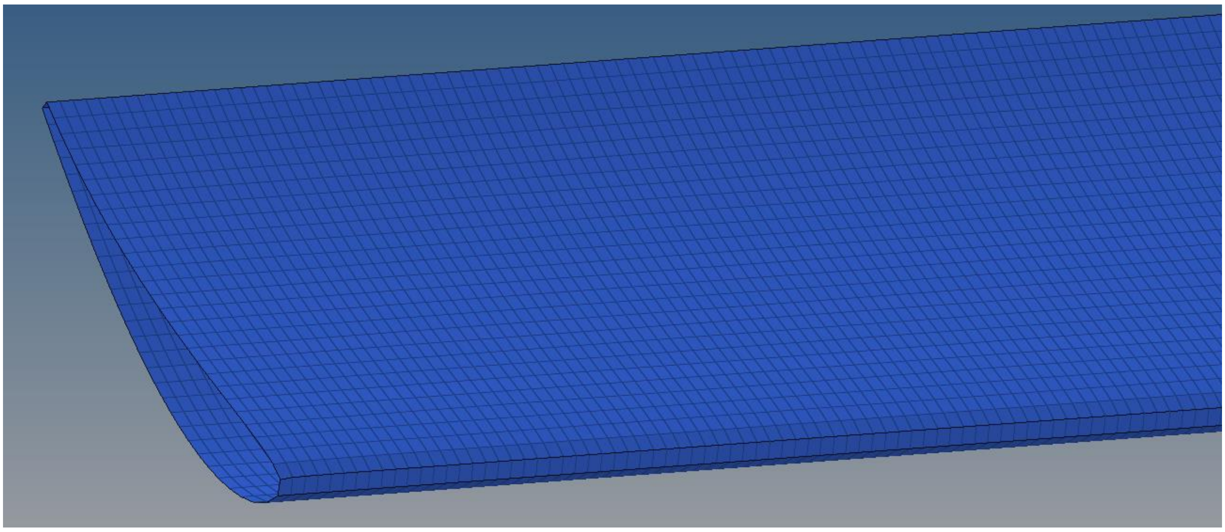

Figure 32. Flaps Mesh

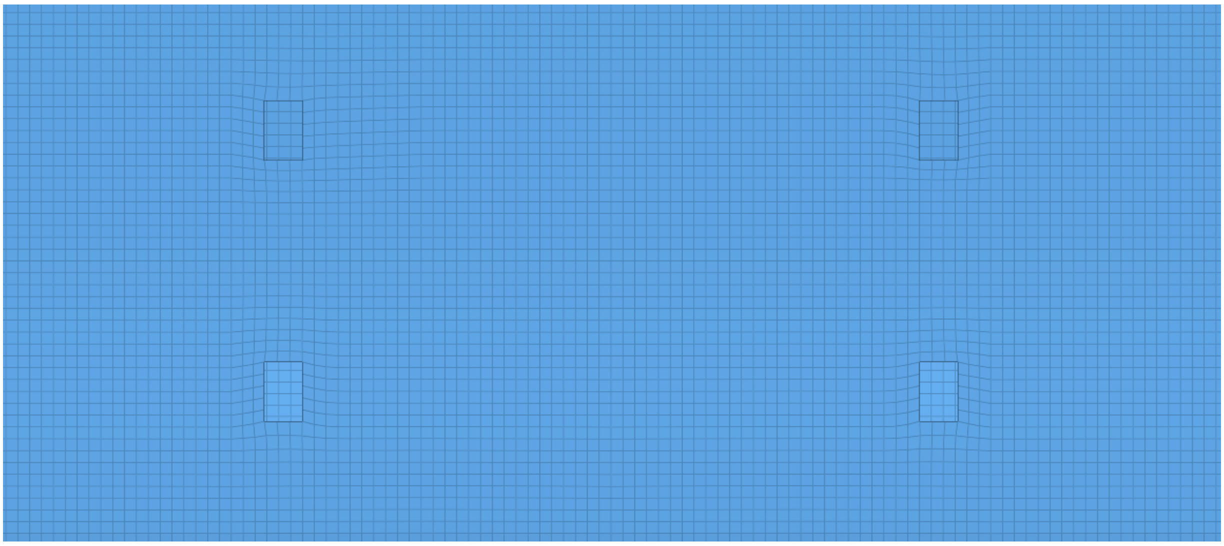

Figure 33. Mainplane holes for the ribs flanges

Ribs

Ribs are modelled as solid components. Their mesh is created starting from the external surface from which is created the 2D mesh. The 3D mesh is created from the 2D mesh, splitting the quad element into tria and creating so a tetrahedral elements mesh. Their geometry is compenetrated into the surface geometry of the wing elements, while the actual geometry has an offset from that surface. This approximation is done only in the numerical model for easiness of modelling because it does not influence the bending behaviour of the wing elements and the component is not critically loaded, therefore no important information is lost in this way.

Inserts

Inserts are made of Rymyc cloth, that is composed by recycled short carbon fibres to be used with resin infusion.

Inserts are modelled as 3D components with orthotropic properties by using the MAT9ORT material card image, since the inserts has different behaviour for the out-of-plane loading direction and the in-plane. More specifically, the out-of-plane direction is the one where the insert is loaded by the bolt compressive force.

Rod and screws

Both rod and screws are modelled as 1D elements with their respective cross section. For the rod (the one connecting the main hoop to the left support to triangulate against lateral loads), CROD elements are used with a tube cross section (D13-d10) to model the tubular part of the body made of carbon fibre. The rodends and the flange to attach the rod to the support (that is glued to the carbon fibre shell) are approximated with a RBE2 element that connect the ends of the rod to the structure to which is connected.

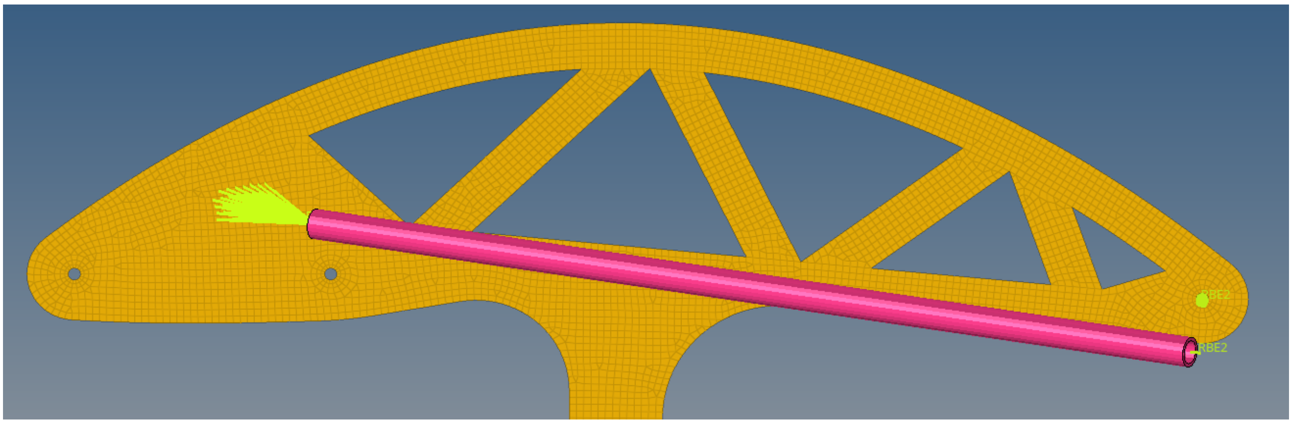

Table 15. Rod modelling

Bolts are modelled as 1D elements as well and are included in the model only the bolts used to mount the supports to verify the effect of the tightening force on the flanges of the ribs and the supports. Since they must withstand shear forces, M5 calibrated bolts are used and are modelled through CBEAM elements to which a pre-tensioning force is applied.
In order to verify the shear strength of the bolts, a simulation was performed in which the supports are approximated as infinitely rigid, so that they can be excluded from the model, and the constraints are applied directly to the flanges of the ribs through an RBE2 element connected to the inner faces of the holes. In this way are obtained the constraint reaction forces that are used for the bolt verification.

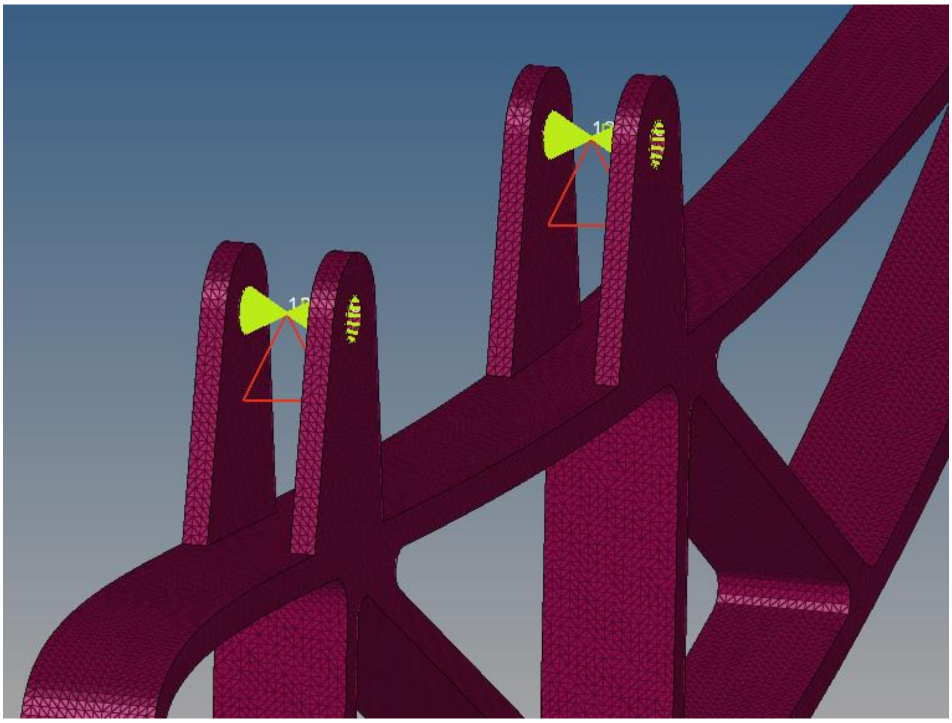

Figure 34. Modelling of constraints for bolts shear verification

3.3.2 Contacts

Forces and moments are transmitted between components by means of contacts. The type used to perform the simulation is FREEZE, a linear static contact that does not allow relative motion between the surface in contact since there is not sliding between the surfaces of the two components in contact.

Contacts are defined between:

- Ribs and outer carbon fibre shell
- Rib and endplates
- Inserts and carbon fibre structure
- Supports ribs and supports

3.3.3 Load cases and constraints

As mentioned earlier, all simulations assumed that the main hoop is vastly rigid compared to the Rear Wing. Consequently, constraints for the model were specifically applied at the mounting point of the support to the Main Hoop, thereby excluding the rest of the vehicle structure from the simulations.

The assembly undergoes analysis across different load cases, with the aerodynamic scenario identified as the most demanding. Compliance with technical inspections necessitates a lower level of mechanical performance.

The structural dimensioning is predicated on the flexural stiffness requirements for the wing element to ensure proper aerodynamic functionality.

Additional load cases were examined to assess the structure's behavior in various potential scenarios beyond the aerodynamic stress.

Constraints

Constraints are applied to the insert hole internal face with an RBE2 element. All the degrees of freedom are locked but the rotations around y-axis since the inserts can rotate around the bolt.

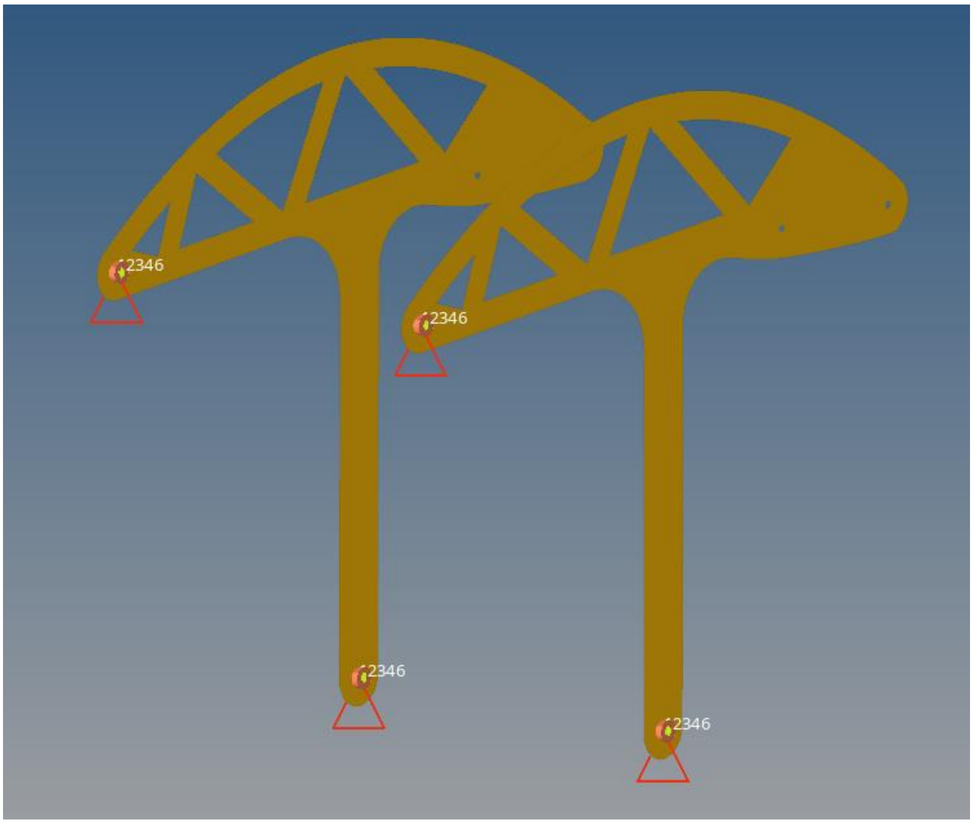

Figure 35. Assembly constraint modelling

Aerodynamic load

To conduct a more comprehensive study of stress and displacement in the mainplane, the FEM modeling geometry must incorporate features such as bolt holes or openings for flange ribs. When simulating aerodynamic loads using a pressure map obtained from CFD analysis, it is crucial that the surfaces do not contain holes. Otherwise, Hypermesh fails to accurately interpolate pressure loads onto the component mesh, resulting in an incorrect summation of forces. If a surface without holes is utilized for FEM analysis the maximum stress is underestimated by 13.5%, as illustrated in the accompanying picture, if a constant pressure load is applied. Displacements, on the other hand, are practically the same.

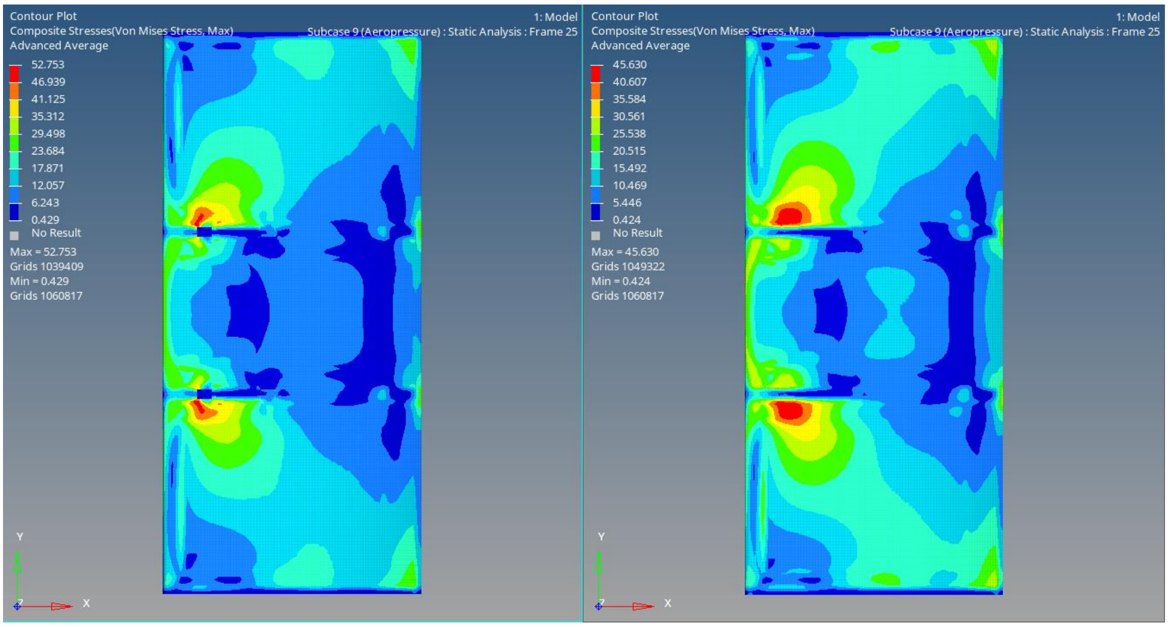

Figure 36. Mainplane stress: surface with openings (left); surface without opening (right)

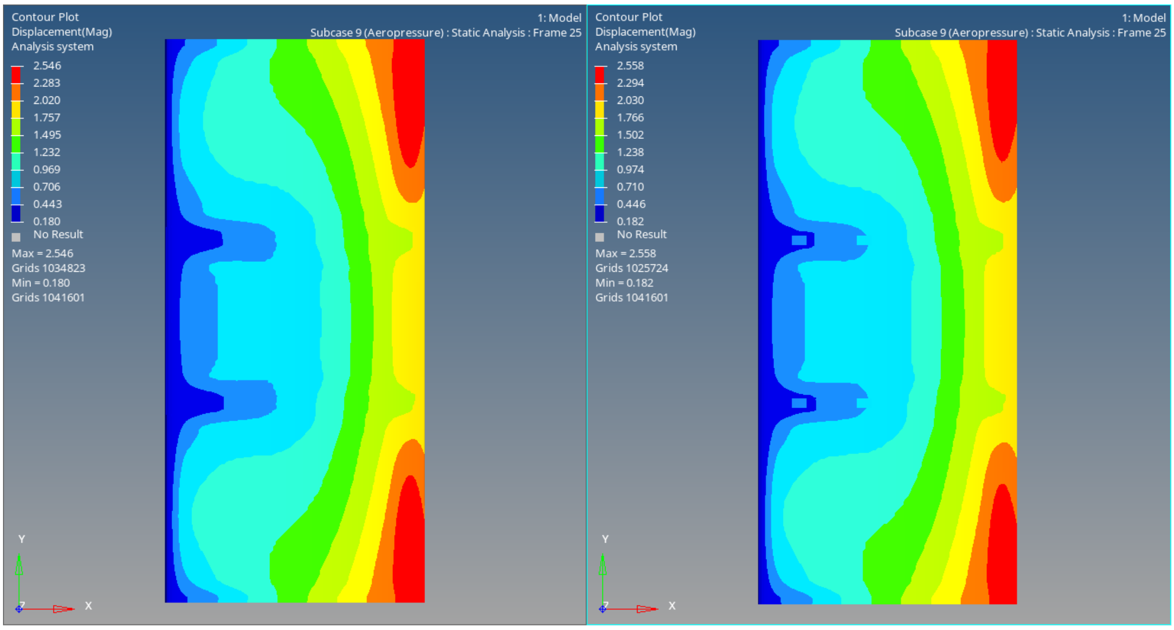

Figure 37. Mainplane displacement: surface with openings (left); surface without opening (right)

An alternative approach to modelling the aerodynamic load involves applying a constant-magnitude pressure to the pressure surface and leading edge of the component. The pressure magnitude is determined by calculating the resultant of the downforce and drag components and dividing it by the area to which the pressure is applied. This method eliminates the requirement for a surface without holes.

The stress and displacement results from both methods of modelling the aerodynamic load show a minimal difference in terms of magnitude, with a maximum variance of 5%. The fields of displacements and stresses are slightly different. Around the supports attachment points, it is evident that in the case of constant pressure distribution, the stresses are higher than in the case of the pressure map, where a smaller pressure is effectively acting on that part because there is a disturbed flow in that area that creates a smaller load than the one approximated by the constant pressure distribution. Same thing happens with the displacements. Instead, going towards the trailing edge, the displacement and stresses between the two load cases are more similar since it's a less disturbed area, confirming that the constant pressure distribution is a good approximation of the pressure map distribution.

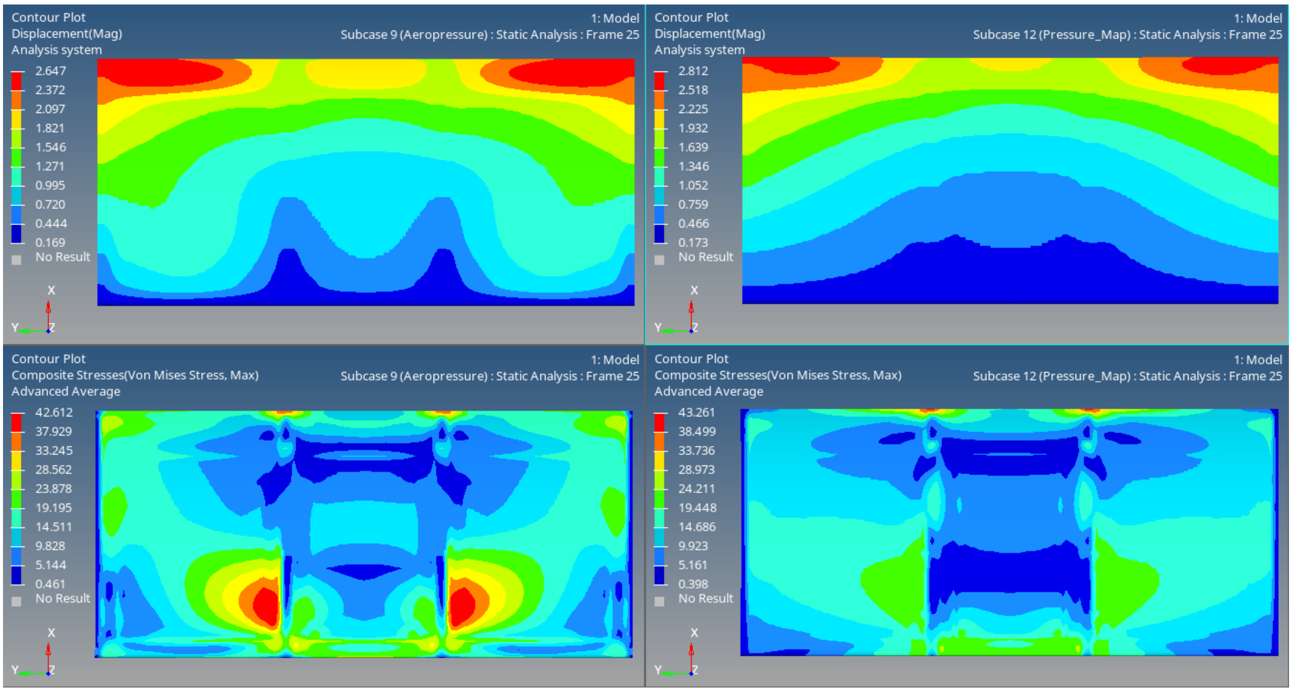

Figure 38. Comparison between Constant pressure (left) and Pressure map (right)

Consequently, the choice to employ the constant-magnitude method for aerodynamic load modelling was based on its user-friendly characteristics, making it a more practical option compared to the method relying on a pressure map.

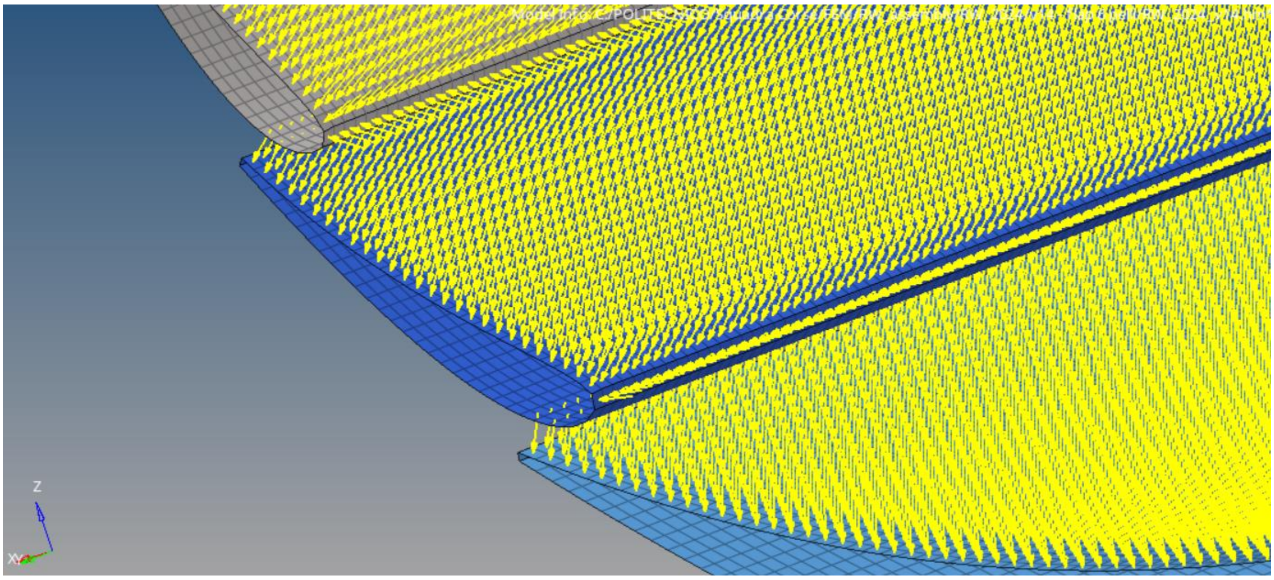
Figure 39. Constant pressure distribution on pressure surface elements

Technical Inspection Load

In the technical regulations of Formula Student, the structural requirements for the aerodynamic devices are the following:

« T8.4.1 Any aerodynamic device must be able to withstand a force of 200N distributed over a minimum surface of 225 cm2 and not deflect more than 10mm in the load carrying direction.

T8.4.2 Any aerodynamic device must be able to withstand a force of 50N applied in any direction at any point and not deflect more than 25 mm.»[1]

In my experience as Technical Scrutineer at Formula Student Netherlands, for the 200N inspection are used two sandbags of 10kg each that are placed on the top surface in the most critical point. So, for a case of a rear wing, sandbags are placed as close as possible to the endplates and to the trailing edge of the wing. So, for the geometry of the 2024 Rear wing, it is probable that the sandbags will be placed in between the Mainplane and Flap 1, or in the mainplane only: since the first case is more severe than the second, only the first one will be simulated.

This technical requirement must be applied as well to the beamwing, because, due its orientation, the 10kg sandbags can be easily placed on it. The load is modelled through a distributed force on an area of 225cm2, as stated in the regulations.

For the 50N technical inspection, the scrutineer checks the aerodynamic package by pushing with its finger in the critical point of the aerodynamic devices and evaluate if, by general feeling, the structure is stiff enough. In the case in which the structure seems to be borderline with the regulation limitations, a 5kg load is applied through a dynamometer to properly evaluate its displacement. In this case the load is modelled with a RBE3 connected to the nodes of a 2x2 element area. The location chosen for the application of this load cases are the more critical one: the endplate edge; the flap trailing edge.

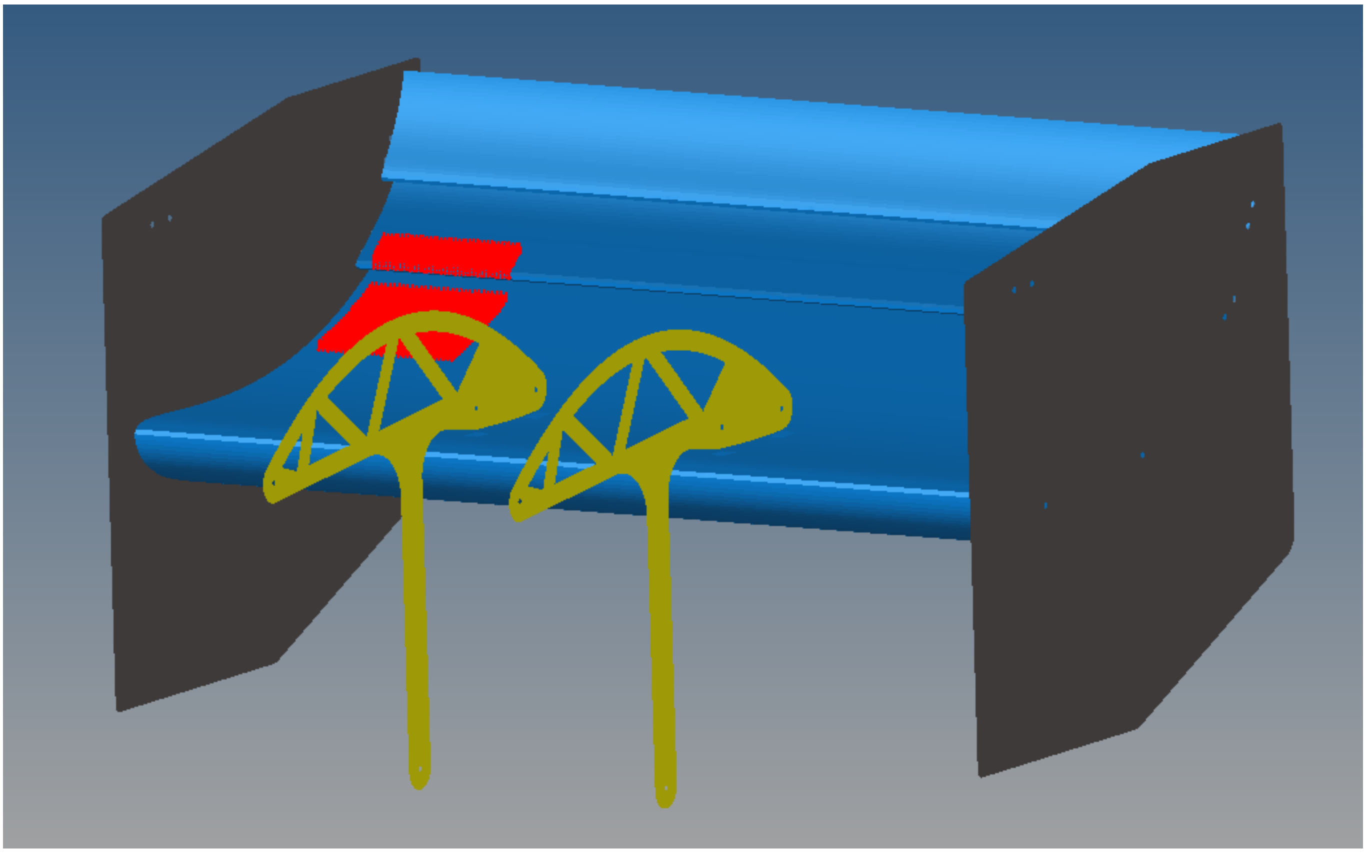

Figure 40. 200N Technical inspection load application on Mainplane (red elements)

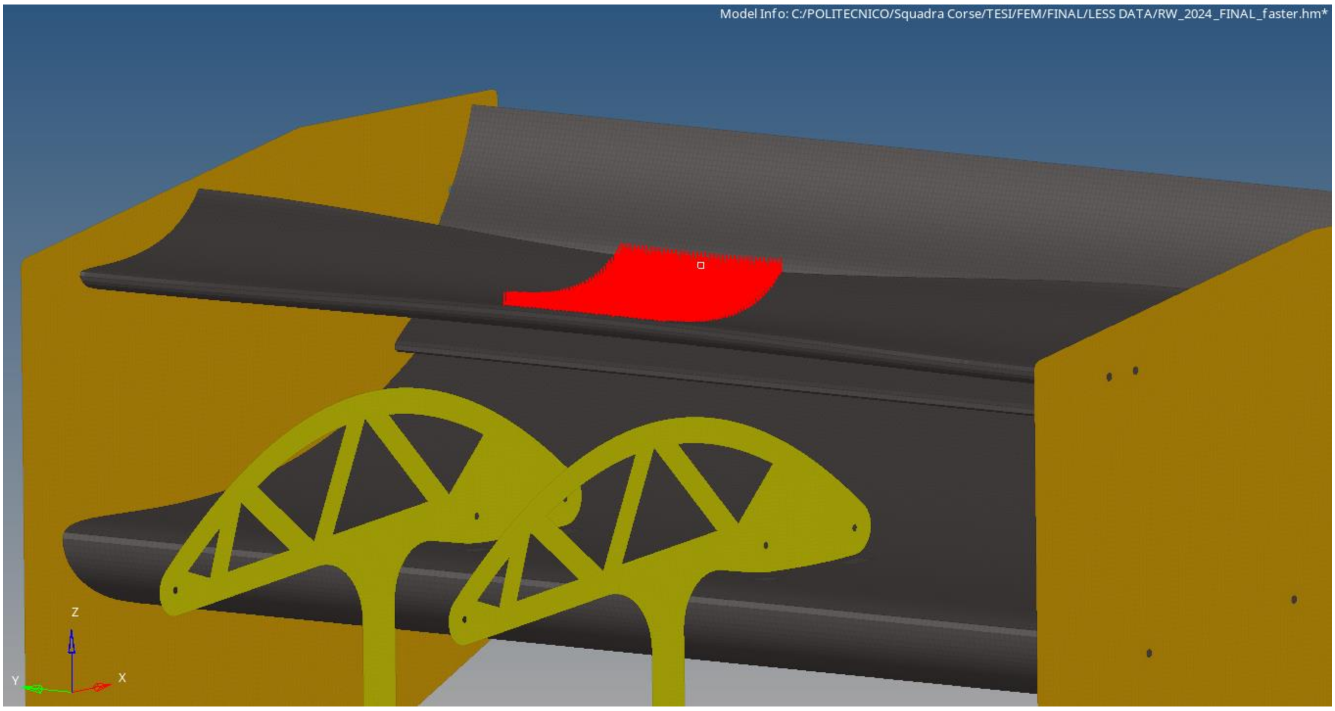

Figure 41. 200N technical inspection load application on Beamwing

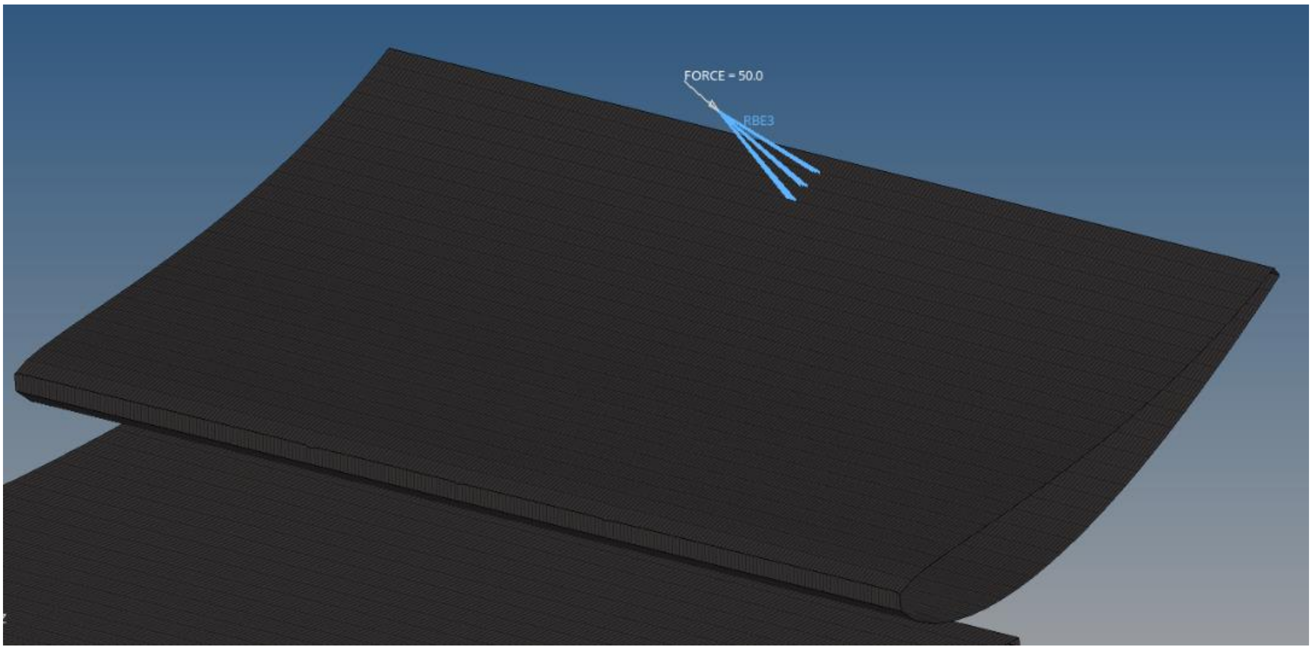

Figure 42. 50N technical inspection load application – Flap TE

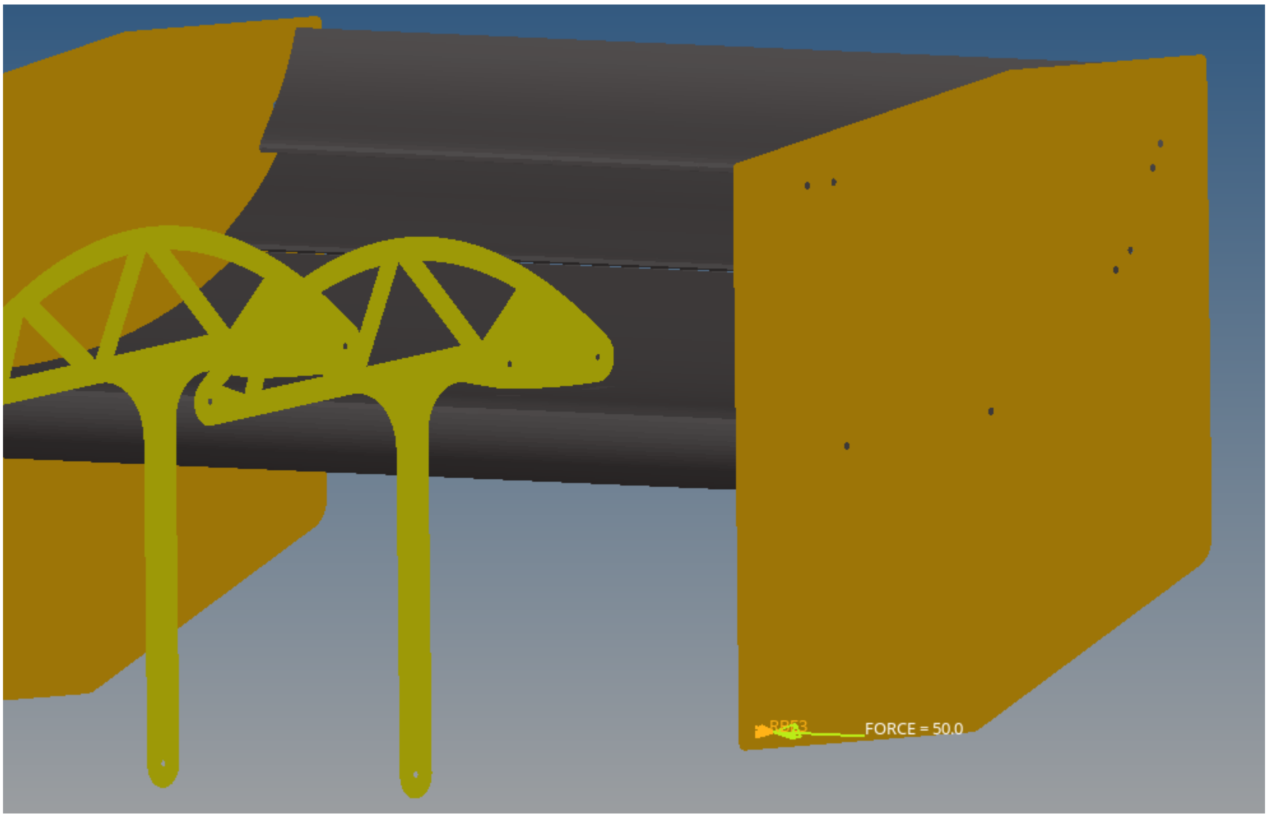

Figure 43. 50N technical inspection load application - Endplate

Lateral loads

In these load cases, lateral forces are applied to the endplate. In the first instance, a 200N force, derived from a CFD analysis involving lateral wind at 120 km/h to replicate the worst-case scenario of the car spinning at top speed, is applied to the endplate as a distributed pressure with a constant magnitude.

This load case serves as a validation for inertial loads during cornering as well. Given that the wing assembly weighs less than 5 kg and the maximum lateral acceleration achievable by the vehicle is less than 3g, the lateral wind during spinning is more severe than the inertial load.

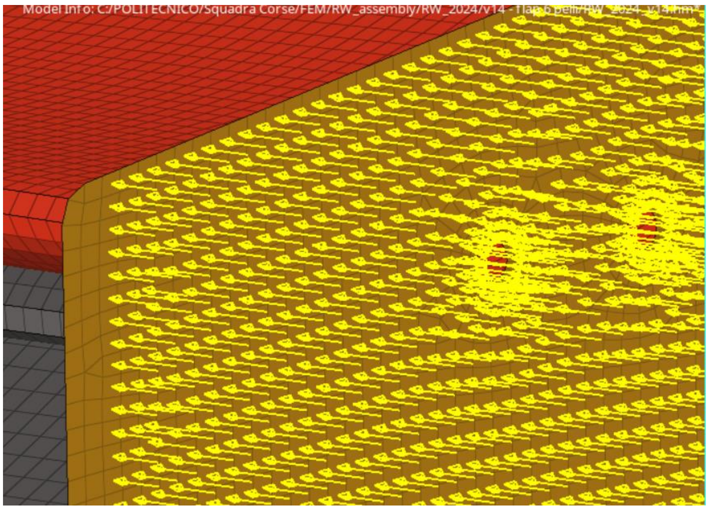

Figure 44. Constant pressure distribution to simulate lateral wind

The second load case applied to the endplate involves a concentrated load of 150N, intended to simulate a scenario where a person incorrectly leans on the wing with his hand. The force is applied to an area of 7x7 cm by means of an RBE3 element.
This is a crucial test to ensure that the structure remains undamaged in the event of such misuse of the wing.

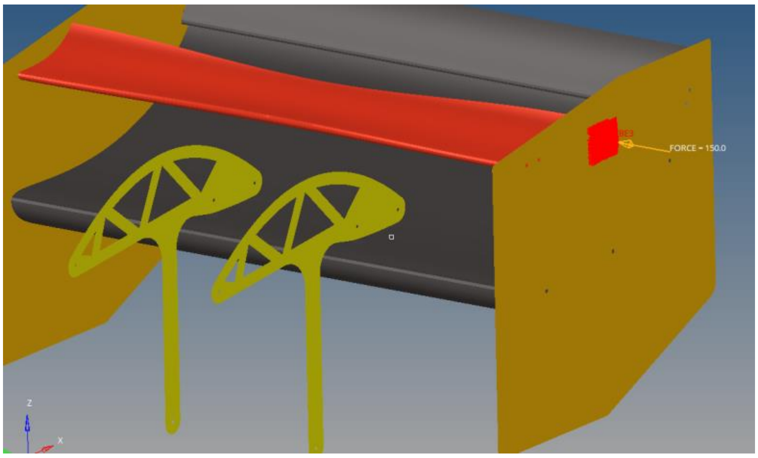

Figure 45. Concentrated lateral force on endplate

Longitudinal force on Flap

As for the concentrated load on the endplate, another verification load case was made where a 150N force is applied to the Flap 2 of the wing, to simulate a person that incorrectly pushes the car from this element as happened to see in some occasions. Force is applied through an RBE3 element on a 7x7cm area.

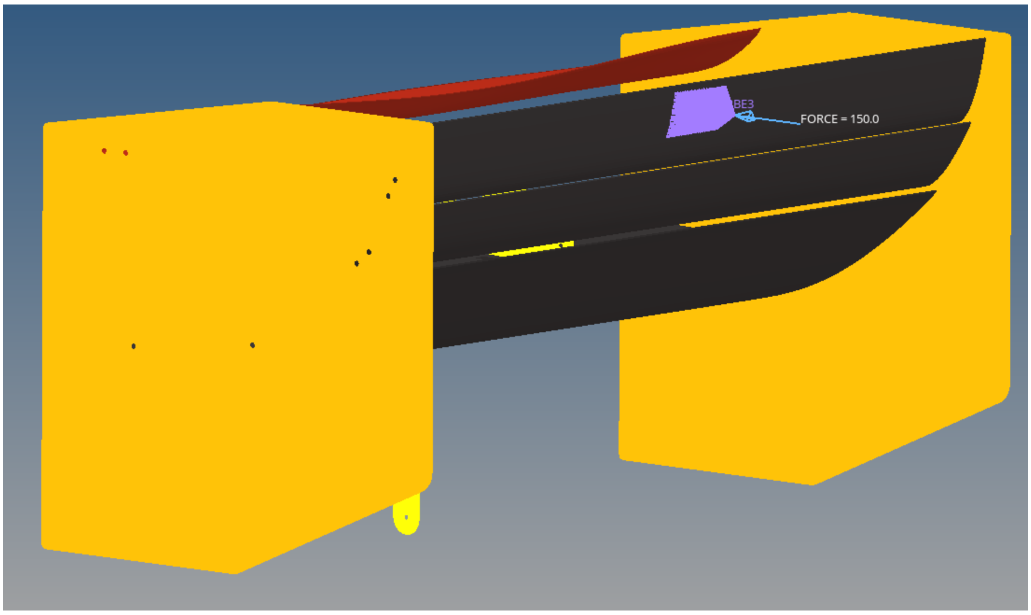

Figure 46. Concentrated longitudinal force on Flap 2

4. Material characterization

This chapter details the comprehensive process undertaken to determine the mechanical properties of the materials used in constructing the Rear Wing assembly, detailing the entire testing procedure, from specimen preparation to the execution of the test.
Given that the carbon fiber originates from project sponsors, Thales Alenia Space and FTS S.p.A., and only superficial density information was initially available, a thorough characterization became imperative to assess the mechanical attributes. The chosen method for this characterization was the traction test, following the guidelines of the ASTM D3039 normative.

4.1 Specimen preparation

According to the normative D3039, specimens recommended dimensions are of 250x25x2.5 mm. Since no information about ply consolidated thickness were available in advance, was supposed a reasonable ply thickness to laminate a slab 2.5 mm thick from which specimens are obtained.
The first type of fabric is a 160gsm 5HS carbon fibre prepreg with Hexcel M18 epoxy resin, a composite fabric developed by Thales Alenia Space. With an estimated thickness of 0.2mm, a 13-ply laminate was created between two steel plates. The resin datasheet recommends an ideal curing process at 180°C and 7 bars for 2 hours. However, the equipment accessible to the team for the curing process can operate up to 150°C and 6 bars, conditions in which the resin can still be cured ensuring good mechanical performances.
For this material, was laminated a slab composed by 13 plies, estimating a ply consolidated thickness of 0.2mm, between two steel plates. The resulting laminate had a thickness of 1.8 ± 0.05 mm, from which 13 specimens of dimensions 250x25mm were obtained using waterjet cutting to ensure acceptable finishing on the side surfaces.

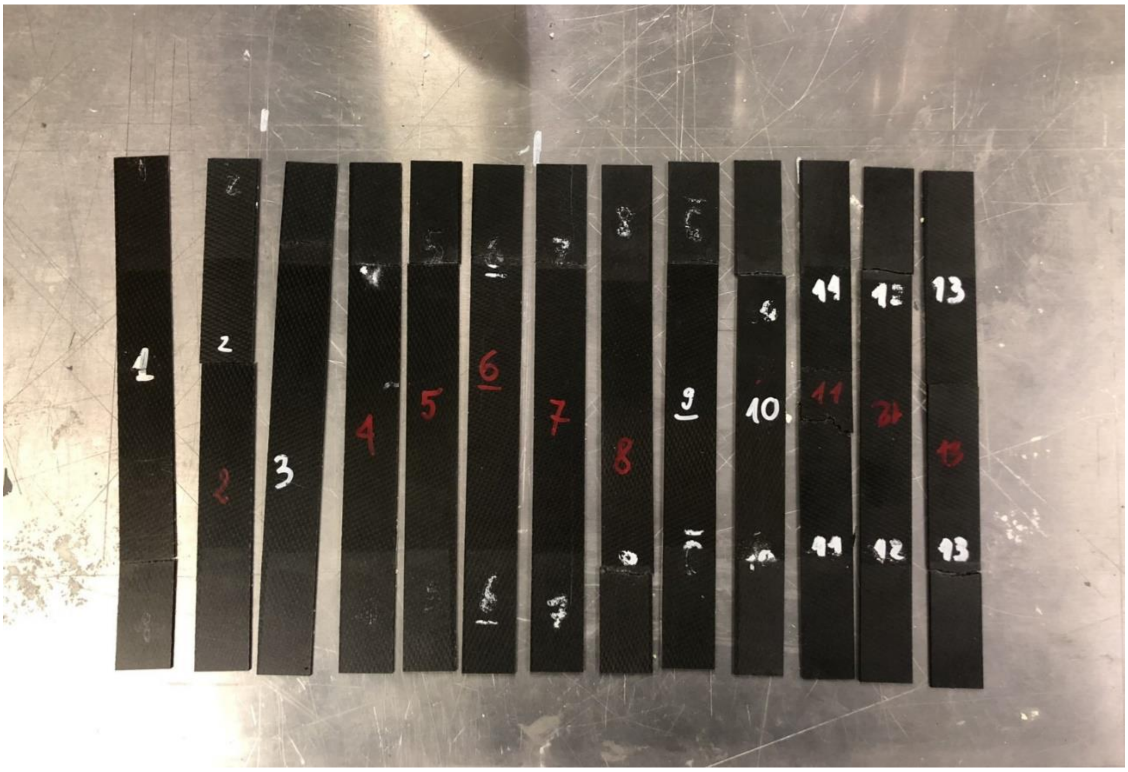

Figure 47. 160gsm 5HS Thales Alenia carbon fibre prepreg test specimens

The second material is a dry fabric of 220gsm twill carbon fibre, provided by FTS S.p.A., with RAKU TOOL EL-2203/EH-2952-1 epoxy resin. For slab manufacturing, the resin infusion technique was chosen. This process allows for better control of the resin quantity absorbed by the fabric compared to wet layup but results in a rough surface on the side not in contact with the steel plate. Twelve plies, with an estimated thickness of 0.23mm, were used, resulting in a thickness of 2.76mm to account for material removal during the sanding process to achieve a smooth surface on the rough side. Surprisingly, a final slab thickness of 3.33mm was obtained.
From the resulting plate, 5 specimens of 205x25mm were obtained through waterjet cut.

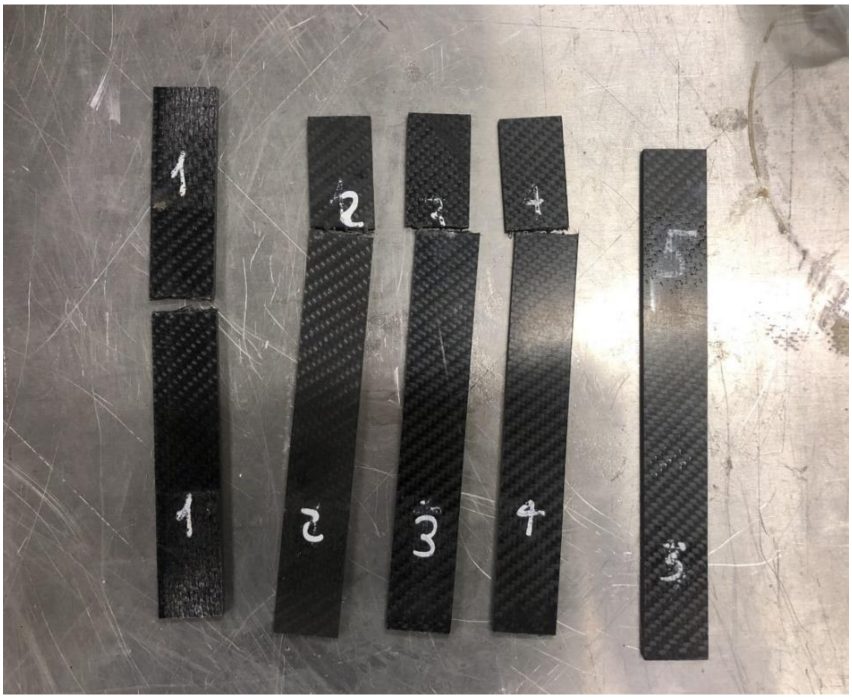

Figure 48. 220gsm Twill FTS carbon fibre test specimens

4.2 Test conduction

The tensile test was conducted in the Fatigue Laboratory of CRF (Centro Ricerche FIAT) with an MTS 100 kN hydraulic machine at a constant strain rate, as stipulated by the relevant standards.

Figure 49. MTS 100kN Tensile test machine

To enhance grip between the clamps and specimens without escalating clamping pressure, 220-grit sandpaper was interposed against the carbon fibre surfaces within the clamps, given that no tabs were employed for the test.
The elastic modulus of the material was measured using an Axial Extensometer in the central section of the specimen.

Figure 50. Traction test setup with axial extensometer

4.3 Test results

Stress on the specimen is computed as:

$$\sigma = \frac{F}{A}$$

where:

- F: is the maximum force before failure
- A: average cross section area

The predominant failure mode observed in most specimens was lateral within the grip area, attributed to excessive interlaminar stresses resulting from clamping pressures. After experimentation, the optimal clamping pressure for the Thales carbon fibre specimen was identified at 80 bars. Initial tests at 60 bars proved inadequate, evidenced by a specimen that started sliding. Consequently, the clamping pressure was increased to 80 bars to mitigate the issue.

There were two specimens that registered a quite lower tensile strength compared to the other. This was attributed to some defects of lamination found on the specimen after failure.

Specimen	Note	Clamping Pressure [bar]	Thickness [mm]	E [Gpa]	Max Stress [Mpa]
1		80	1.84	100191.3	280.40
2		80	1.87	104988.5	615.20
3		80	1.78	99689.4	572.93
4		80	1.83	102258.2	417.01
5		80	1.8	102915.6	564.71
6		80	1.85	99567.1	508.38
7		80	1.8	102303.3	397.95
8		80	1.77	106362.9	475.66
9		80	1.85	100983.0	273.03
10		60	1.75	109327.6	512.00
11		60	1.78	106148.3	552.03
12	Sliding	60 -> 80	1.86	103114.3	434.57
13		80	1.83	104148.5	495.19

Table 16. 160gsm 5HS prepreg Traction Test summary

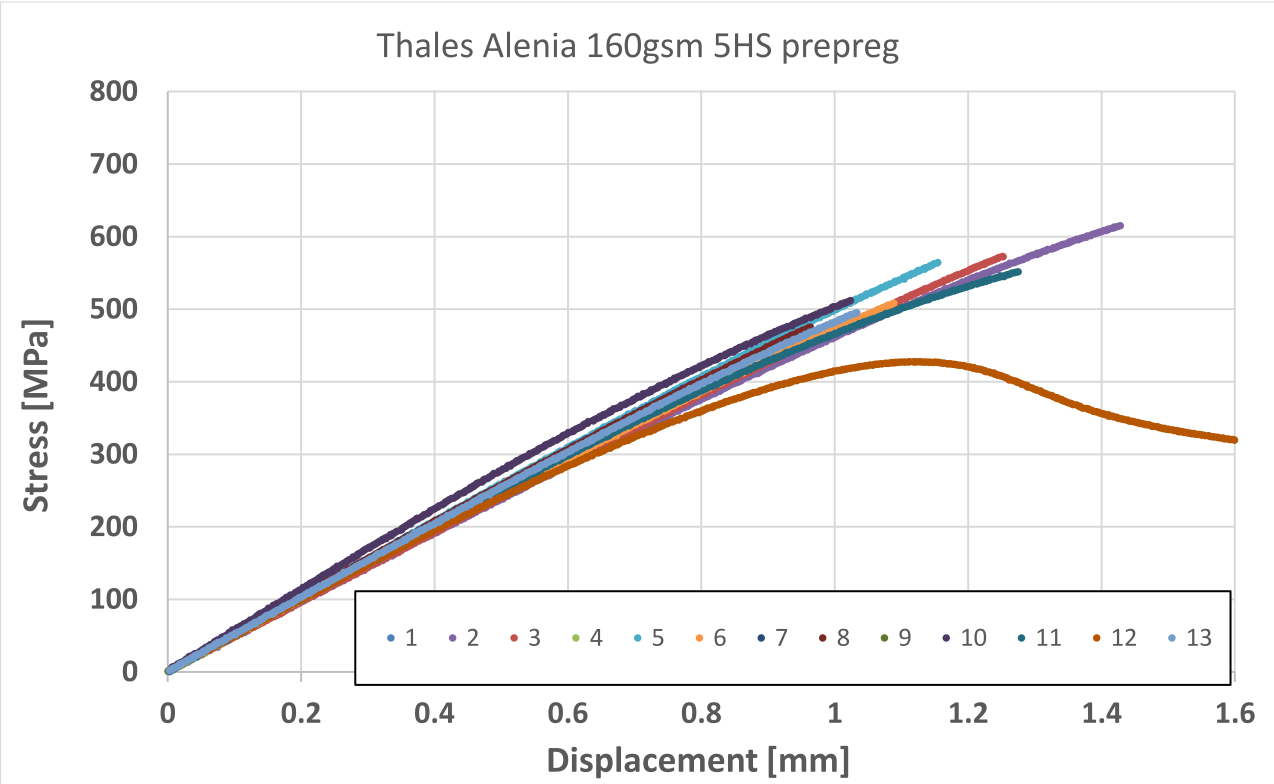

Figure 51. 160gsm 5HS prepreg Traction test results

Specimen	Note	Clamping Pressure [bar]	Thickness [mm]	E [GPa]	σ [Mpa]
1	Sliding – test cancelled	80	3.4		
2		120	3.37	43.1691	506.46
3		120	3.24	46.0551	482.85
4		120	3.03	49.0455	431.27
5	Stopped at 49kN	120	3.33	44.0714	565.30

Table 17. 220gsm Twill fabric tensile test summary

Figure 52. 220gsm Twill fabric Tensile test result

Material properties are then obtained by an average of the experimental result of the tensile test.

For the calculation of tensile strength of the Thales Alenia prepreg carbon fibre, were excluded from the average the two values of the specimen that presented defects of manufacturing, otherwise they would affect the result by underestimating the material performances.

Ply thickness was computed as an average of the specimens thicknesses and divided by the number of plies used for the slab production.

The young modulus of the component is, instead, directly measured on the specimens by means of the Axial Extensometer MTS 634.31F-24. In the table below are resumed the material properties obtained from the test.

Material	**Elastic modulus [GPa]**	**Tensile Strength [MPa]**	**Ply thickness [mm]**	**Material density [g/cm3]**
Thales Alenia 160gsm 5HS prepreg	103.231	504.15	0.14	1.26
FTS 220gsm Twill fabric	45.585	496.5	0.27	1.87

Table 18. Carbon Fibre tensile test result

5. Experimental test

This chapter presents the design of an experimental test, which execution is not part of this work, and the numerical model of it to obtain an expected result.
To enhance the quantitative structural design of these components, it is imperative to establish a correlation between the numerical model employed for simulations and the actual behaviour of the components. To achieve this, an experimental test has been conceived, which will be conducted at the Fatigue Laboratory of Centro Ricerche FIAT, focusing on a flap of the rear wing assembly. This experimental test aims to provide more accurate insights into the structural behaviour of the component, allowing for a refined dimensioning of the structure through FEM anlysis that considers any inaccuracies in the model's estimation of the component's behaviour. The outcomes of this experimental test will contribute to a more robust and reliable structural design.

5.1 Test setup

The proposed test involves a single flap assembly securely fastened to two 10mm thick steel plates through two bolts on each side, mimicking the mounting configuration on the endplates. Subsequently, these two steel plates are affixed to four M20 bolts, which, in turn, are clamped to two cast iron angle plates with T-slots. The angle plates are firmly fixed on a T-slotted cast iron rigid floor. This ensures that any deflections recorded during the test remain uninfluenced by the mounting structure, as the latter possesses higher stiffness in comparison to the flap assembly.
A load is applied by suspending a weight from the flap, utilizing a 3D printed airfoil-shaped block. The block is designed to conform to the curvature of the flap on one side, ensuring uniform load distribution. On the other side, it features a flat shape with a midplane slot through which a wire passes to suspend the weight.

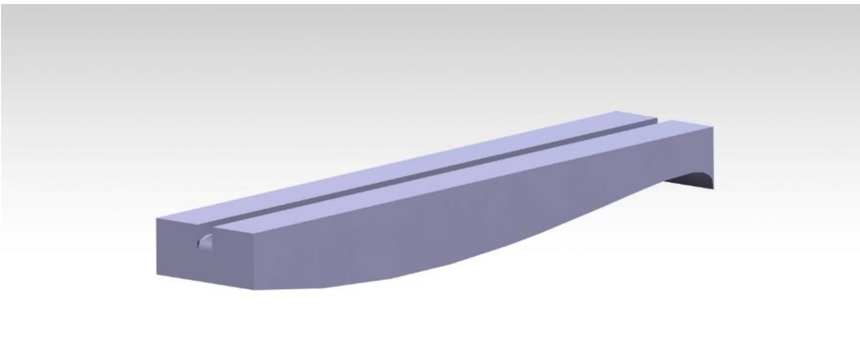

Figure 53. 3D printed block for weight application

The weight can be a 10kg kettlebell or a gym disc, chosen for ease of acquisition, but it can be substituted with any weight that can be hung through a wire or a rope, fitting within the available space inside the mounting structure.
Given that the expected displacement resulting from the weight application is in the order of a few millimetres, a centesimal comparator is employed to measure the flap deflection with reasonable accuracy. The instrument is affixed to the floor, and the measuring pin is placed

against the suction surface of the flap. By precisely determining the point where the comparator is situated, the corresponding mesh element can be identified along with its displacement. This allows for a direct comparison between the actual measured displacement and the numerically estimated one.
A representative preview of the test setup is depicted in the accompanying picture.

Figure 54. T-slot angle plates on T-slot floor

Figure 55. Centesimal comparator used to measure deflection of the flap

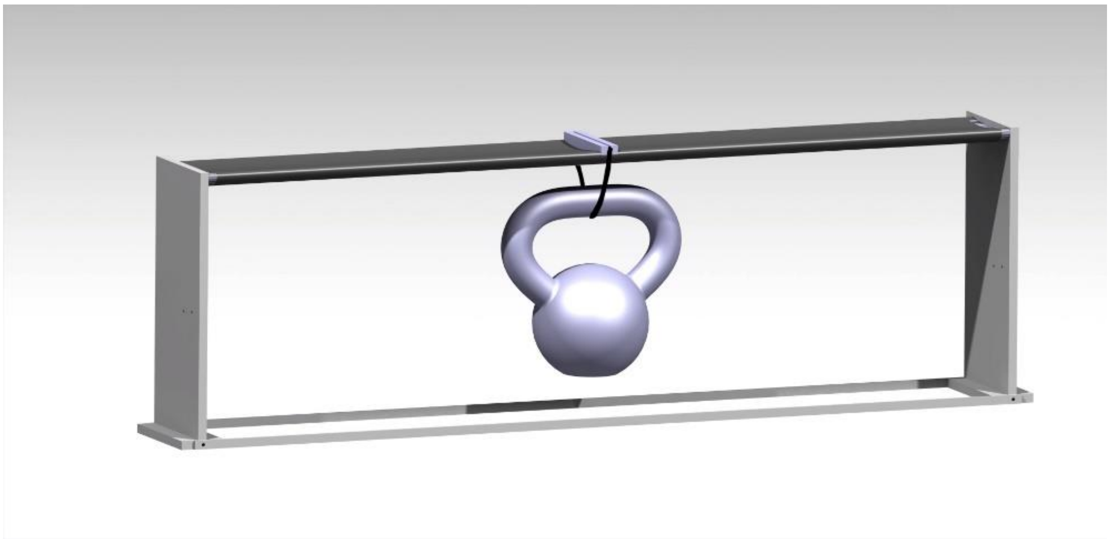

Figure 56. Schematic representation of the experimental test

5.2 Numerical model of the test

For this numerical model, actual geometries of the ribs, considering the carbon fibre shell thickness, is used. It is assumed that the flap outer shell is made up by 3 plies of FTS 220gsm Twill fabric, therefore a 0.81mm gap is present between the rib and the flap surface.
It is reasonable to assume that all the deformation is absorbed by the flap structure since it is the component with smallest stiffness. Because of that, in the numerical model, only the flap surface and the ribs are included, because the structure to which they are attached is assumed to be infinitely rigid.
Constraints are applied to the internal faces of the ribs holes, therefore the bolt deformations are not included in the numerical model because the ribs is absorbing the deformation being of aluminium while the bolt is made of steel. Moreover, since the objective of this study is to establish a correlation between the numerical model used for the structural analysis and the real behaviour of the component, this modelling approach is the same of the one used for the analysis of the Aerodynamic assembly.

Figure 57. Geometry used for the numerical model of experimental test

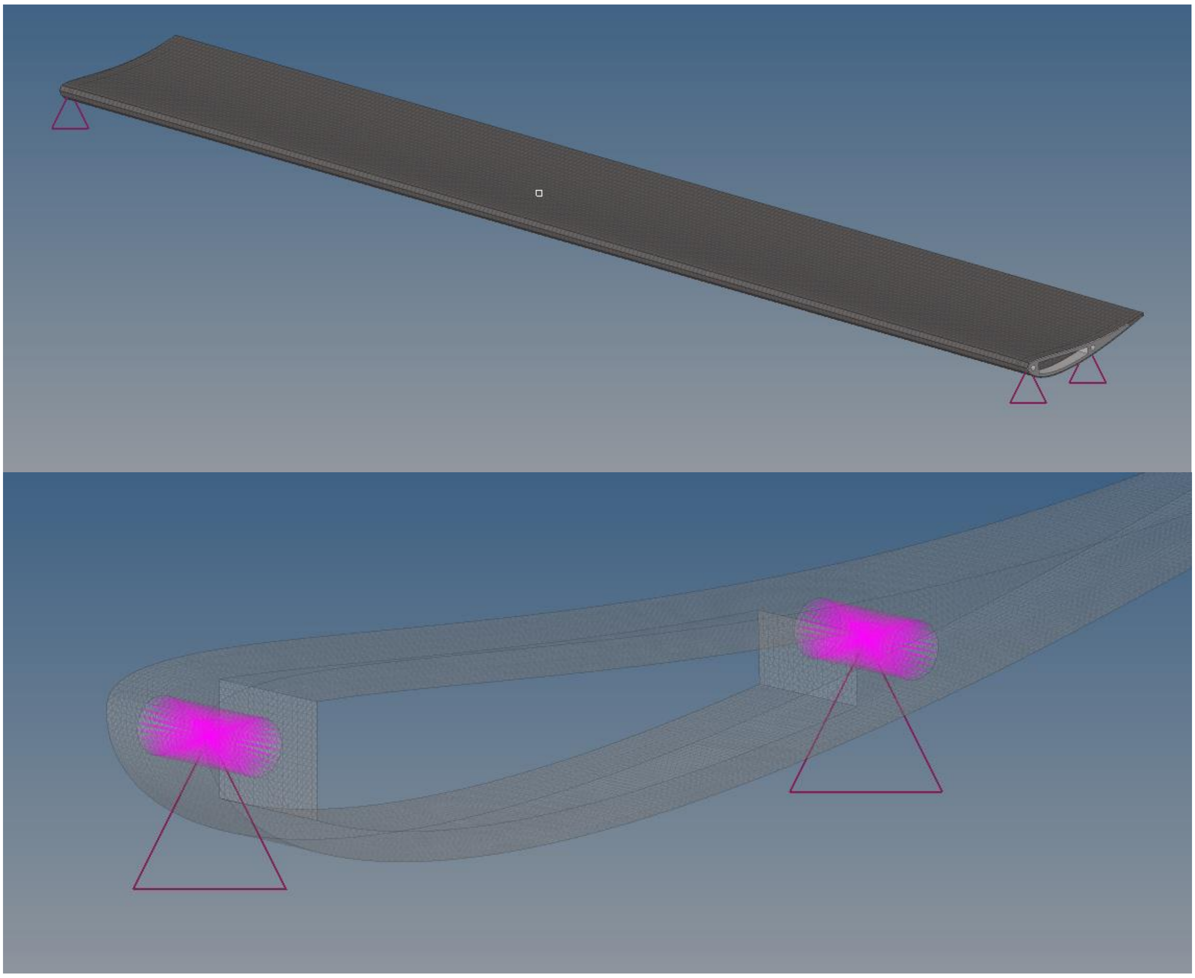

Figure 58. Constraint modelling of the experimental test

The weight applied to the flap is modelled with a distributed force of 98.1 N of an area corresponding to the contact area between the flap and the 3D printed block to which the weight is hung.
The attended maximum displacement is of 4.95mm in the middle of the flap (480 mm from one end of the component).

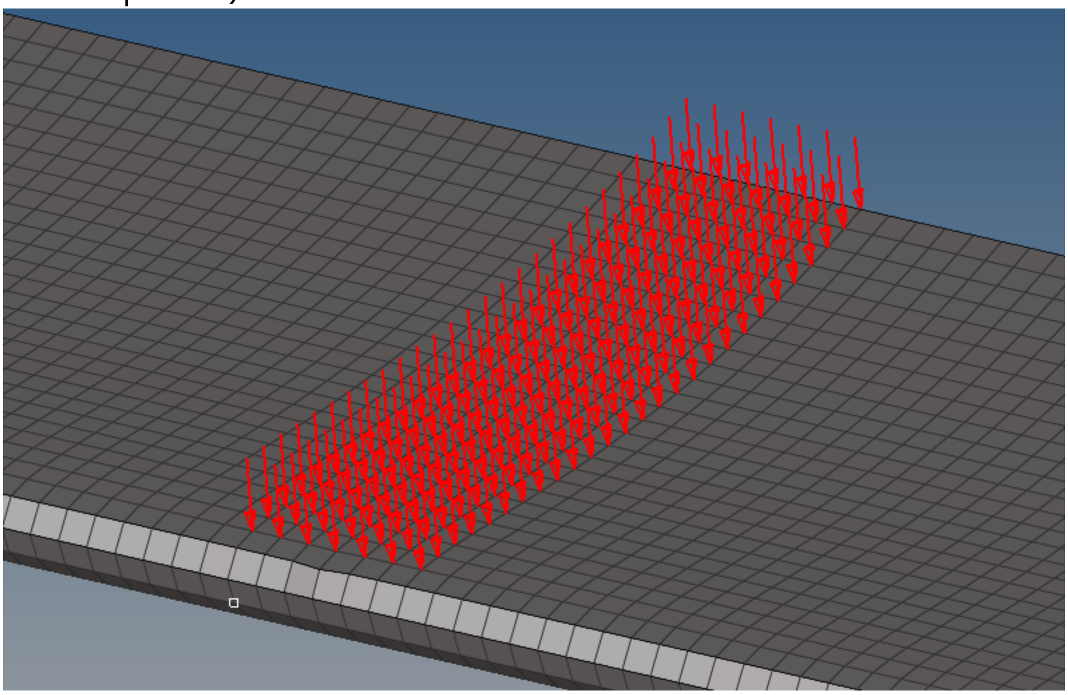

Figure 59. Numerical modelling of the weight application

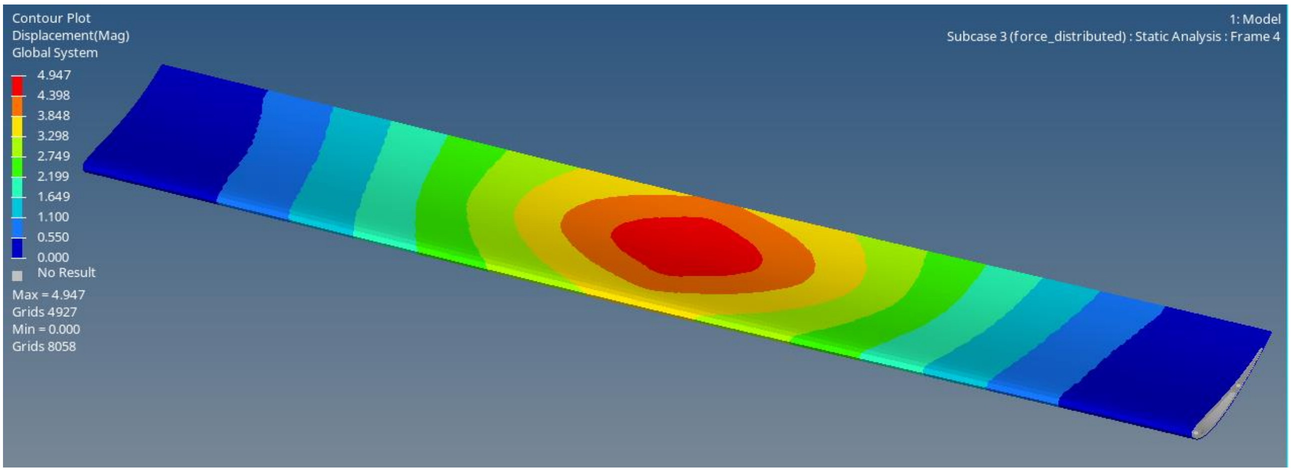

Figure 60. Displacements result of the numerical model of the experimental test

6. Results

In this chapter, the results of the numerical simulations for the load cases outlined in Chapter 3 are presented. The methodology employed to determine the final laminate configuration for the structural design of the wing is also detailed.

6.1 Aerodynamic load

Aerodynamic load is simulated through distributed pressure with constant magnitude with the mainplane surface with the opening for the rib flanges. This load case resulted to be the most critical one, therefore the dimensioning of the components is done considering only the aerodynamic load. Beamwing is the only exception, because for this element the most critical case is the technical inspection of 200 N, that is applied entirely to this element since it has the minimum surface requirements and the sandbags can be easily placed on it.

The target for the dimensioning is the maximum deflection that components can have, to ensure proper functioning of the assembly from an aerodynamic point of view.

The target is to have a maximum displacement of 2mm, in the numerical simulations, at a vehicle speed of 60km/h.

Most critical components for this analysis are the first and second flap, since are the one that bends most of all under the aerodynamic load.

For this component, 3 plies proved to be sufficient for achieving the desired results. Reducing it to only 2 plies would result in an excessive increase of the displacements.

For the supports, was chosen a configuration of 9 plies per side of the panel since a reduction of the layers results in a too large grow rate of stress and displacement.

For the mainplane, that is the most loaded component and the most important one from an aerodynamic point of view, for its dimensioning was chosen a more conservative approach to have a higher stiffness and so a better stability of aerodynamic performances. Therefore, 3 plies of carbon fibre are chosen for this component.

The beamwing is the element subjected to the smallest aerodynamic load, and because of that only 2 plies are sufficient to achieve good aerodynamic performances.

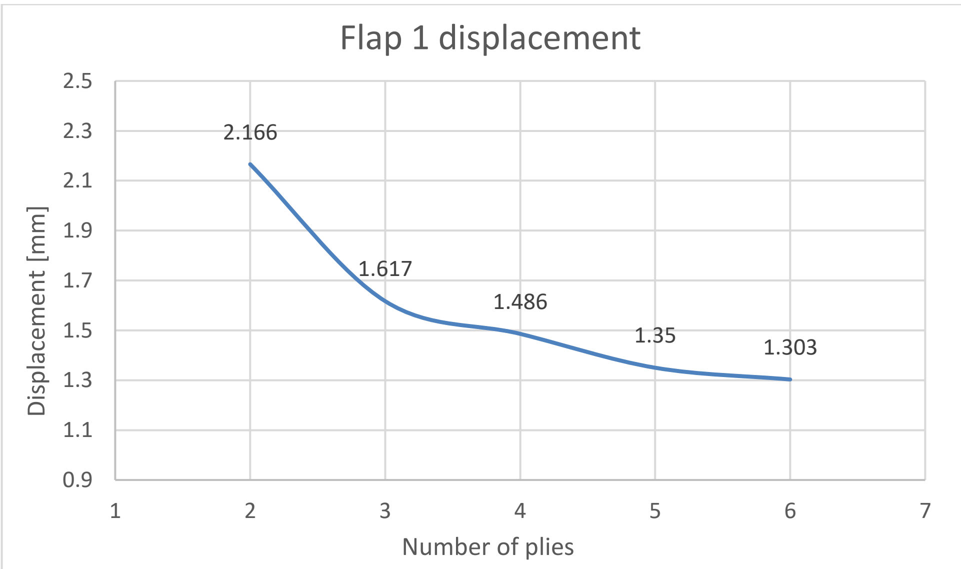

Figure 61. Flap 1 Aerodynamic load displacement as function of plies number

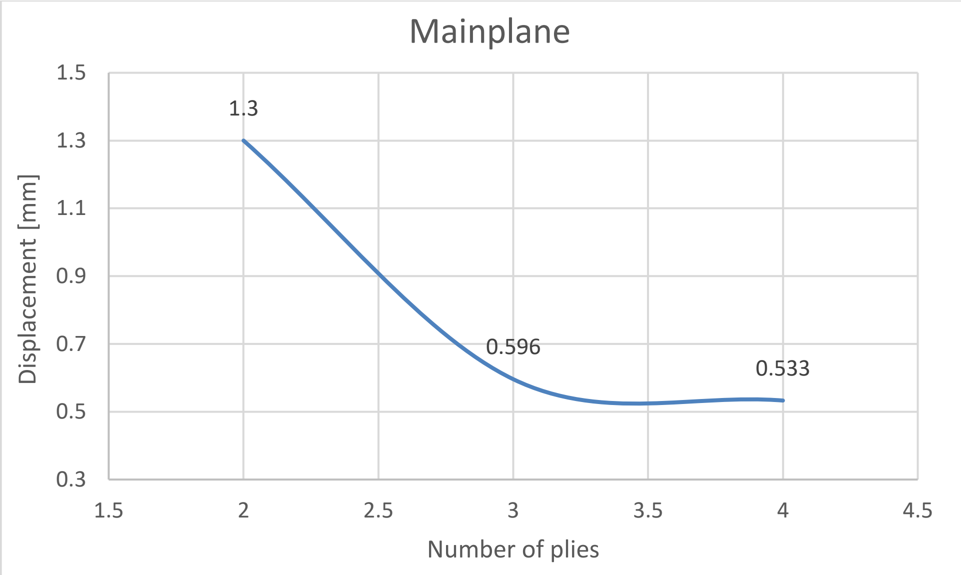

Figure 62. Mainplane Aerodynamic load displacement as function of plies number

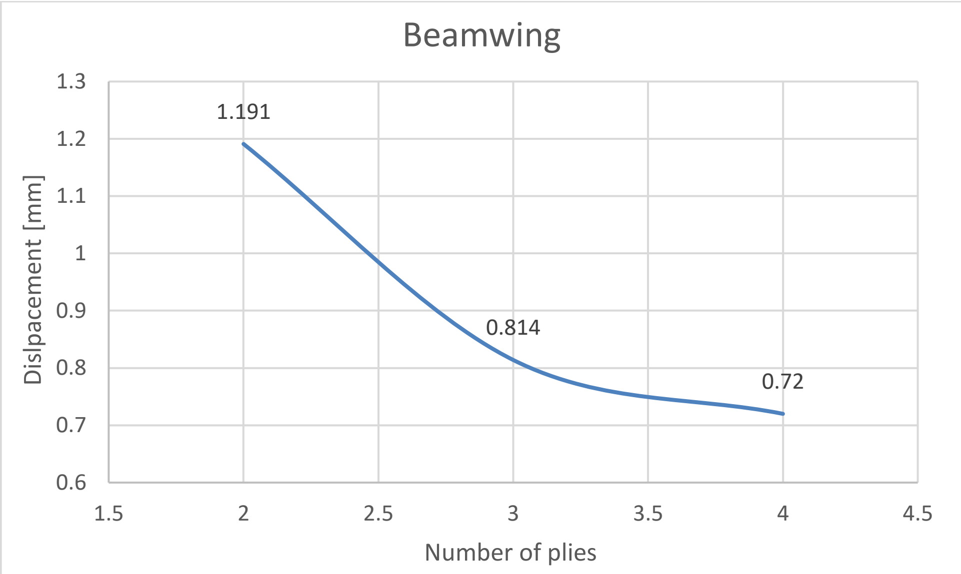

Figure 63. Beamwing Aerodynamic load dispalcement as funtion of plies number

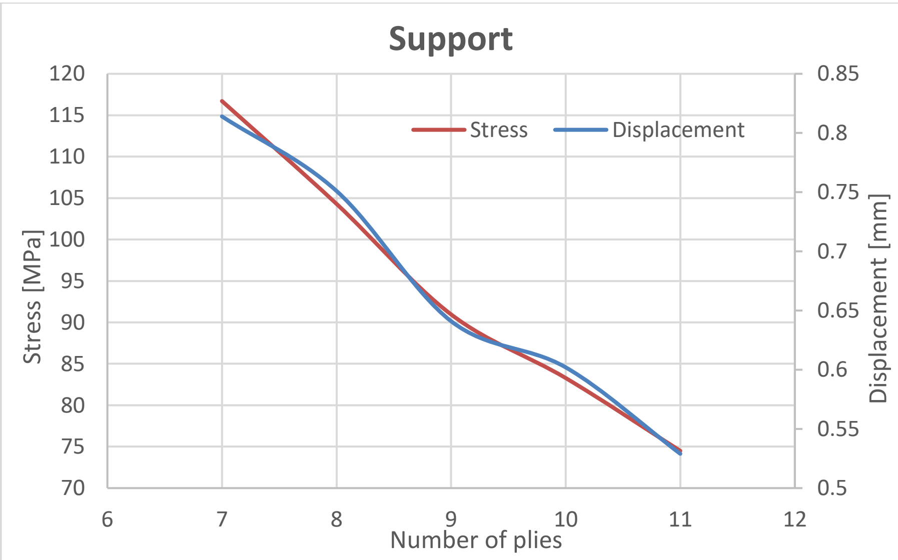

Figure 64. Support Aerodynamic load stress and displacement as function of plies number

Component	Number of plies	Displacement [mm]		
		60 km/h	90 km/h	120 km/h
Mainplane	3	0.604	1.345	2.423
Flap 1	3	1.617	3.636	6.504
Flap 2	3	1.501	3.396	6.089
Beamwing	2	1.191	2.691	4.876

Table 19. Aerodynamic load displacements

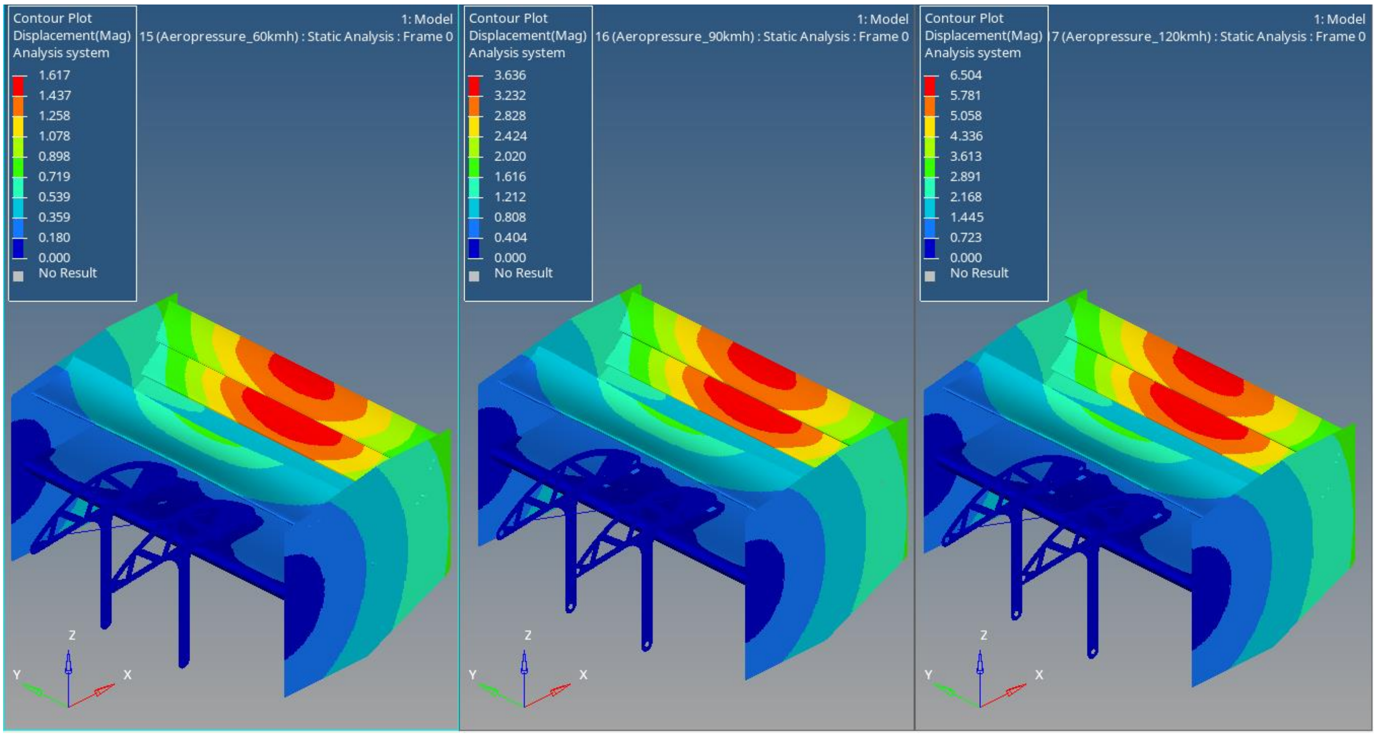

Figure 65. RW 2024 - aerodynamic load displacement at 60 km/h (left), 90 km/h (centre), 120 km/h (right)

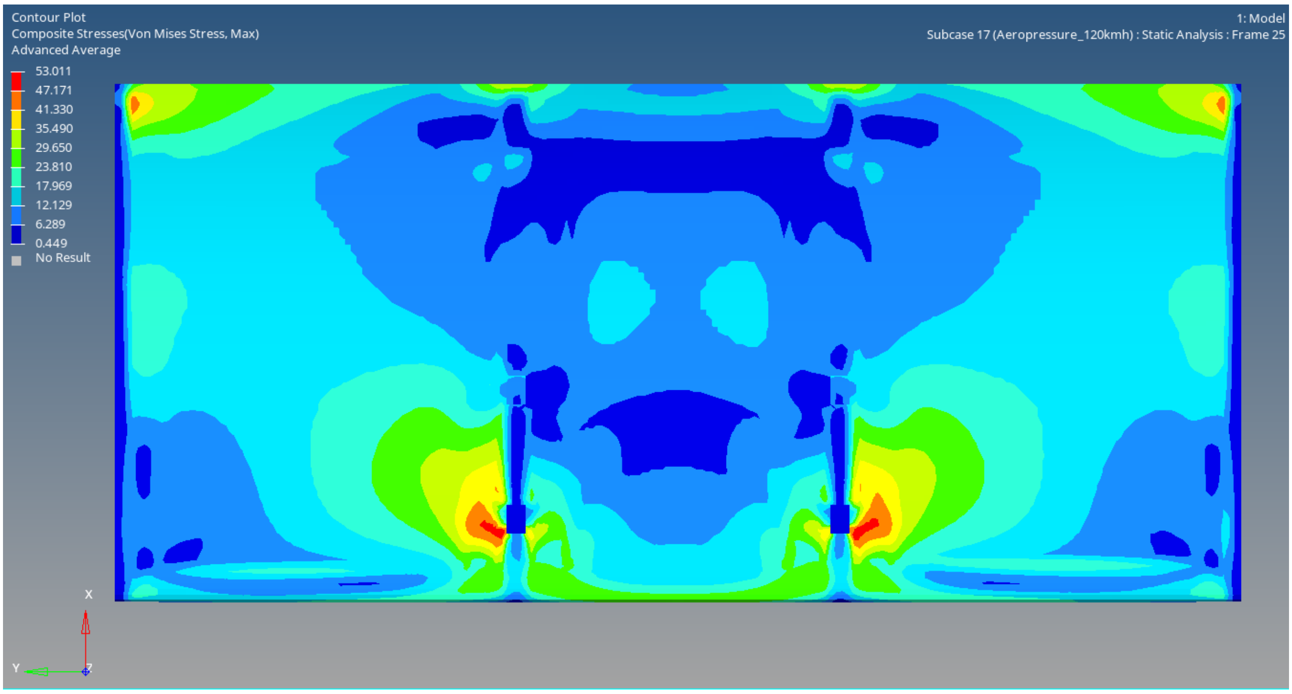

Figure 66. Mainplana - Aerodynamic load stress

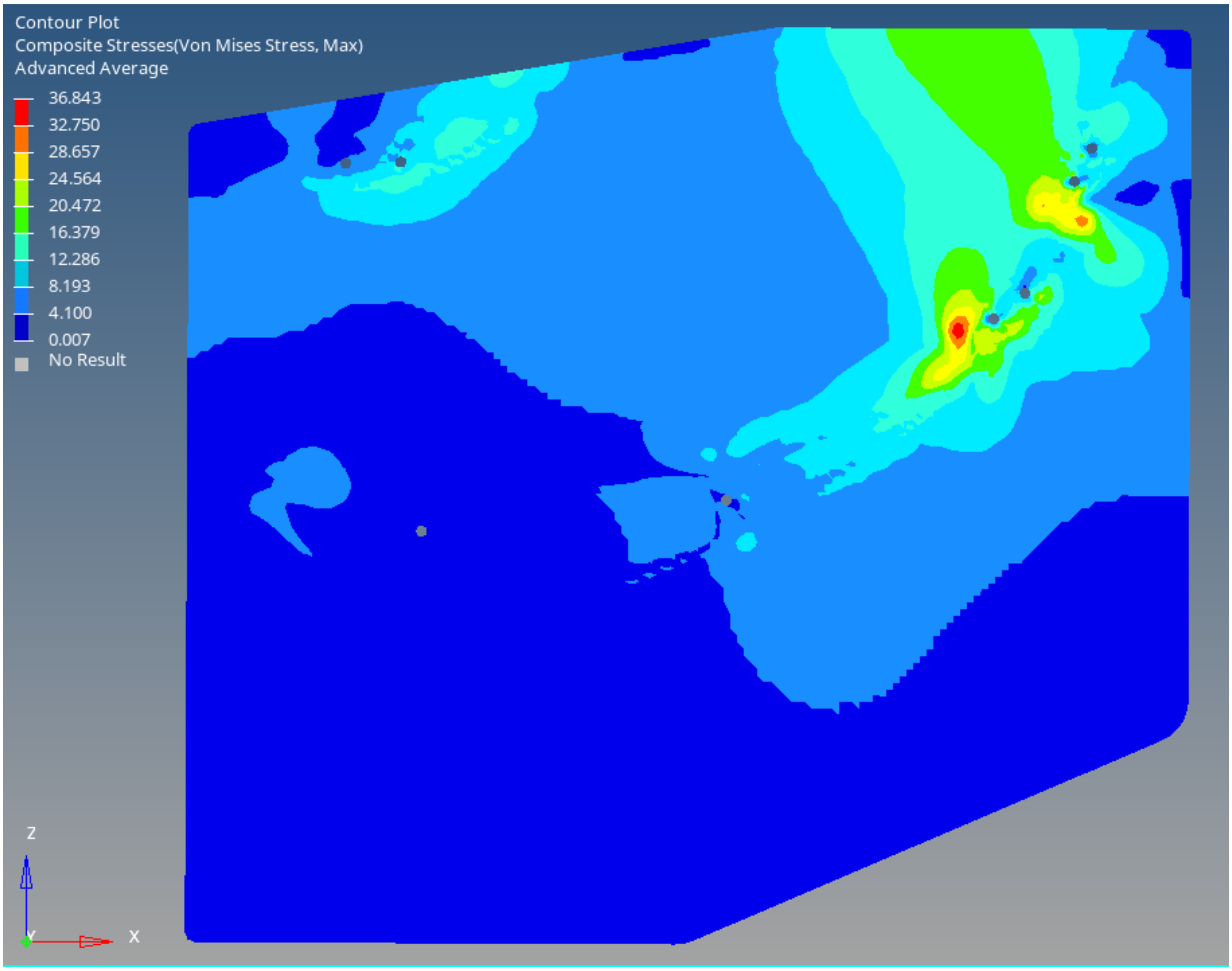

Figure 67. Endplate - Aerodynamic load stress

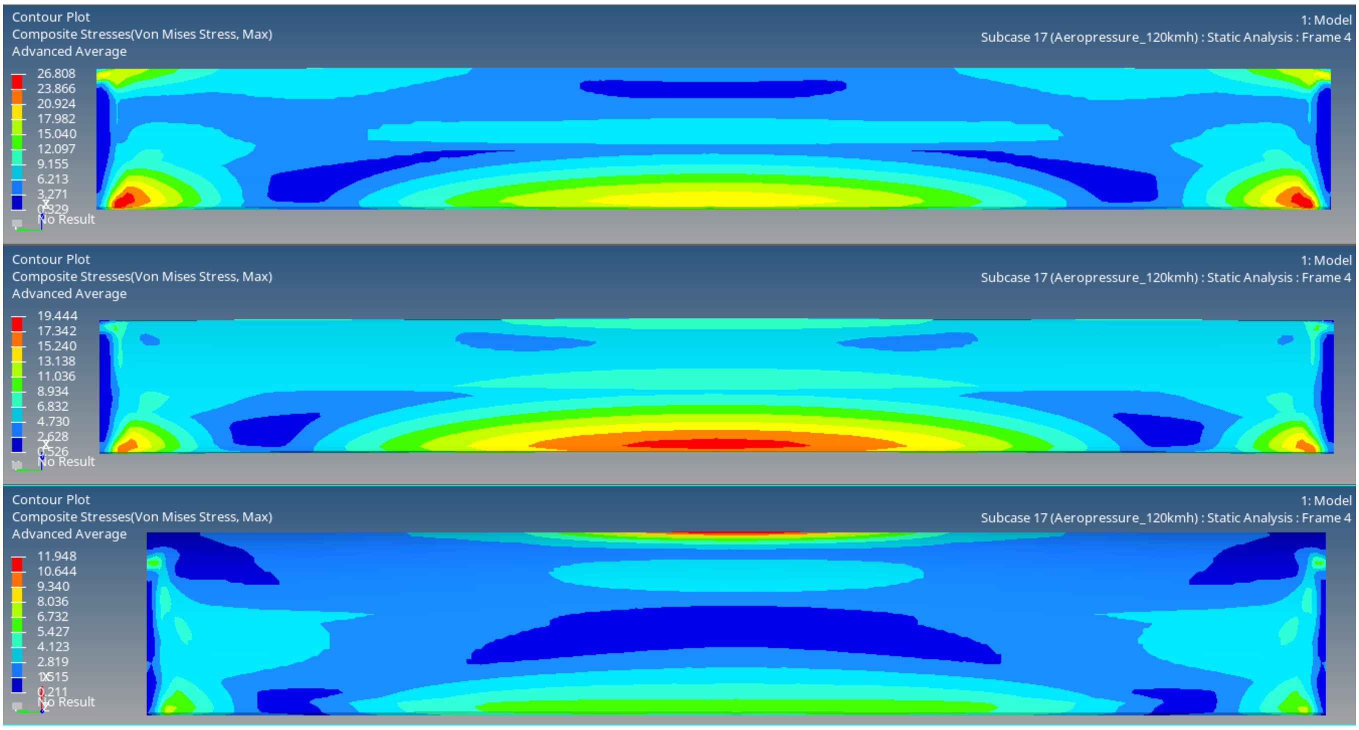

Figure 68. Flap 1 (top); Flap 2 (centre); Beamwing (bottom) - Aerodynamic load stress

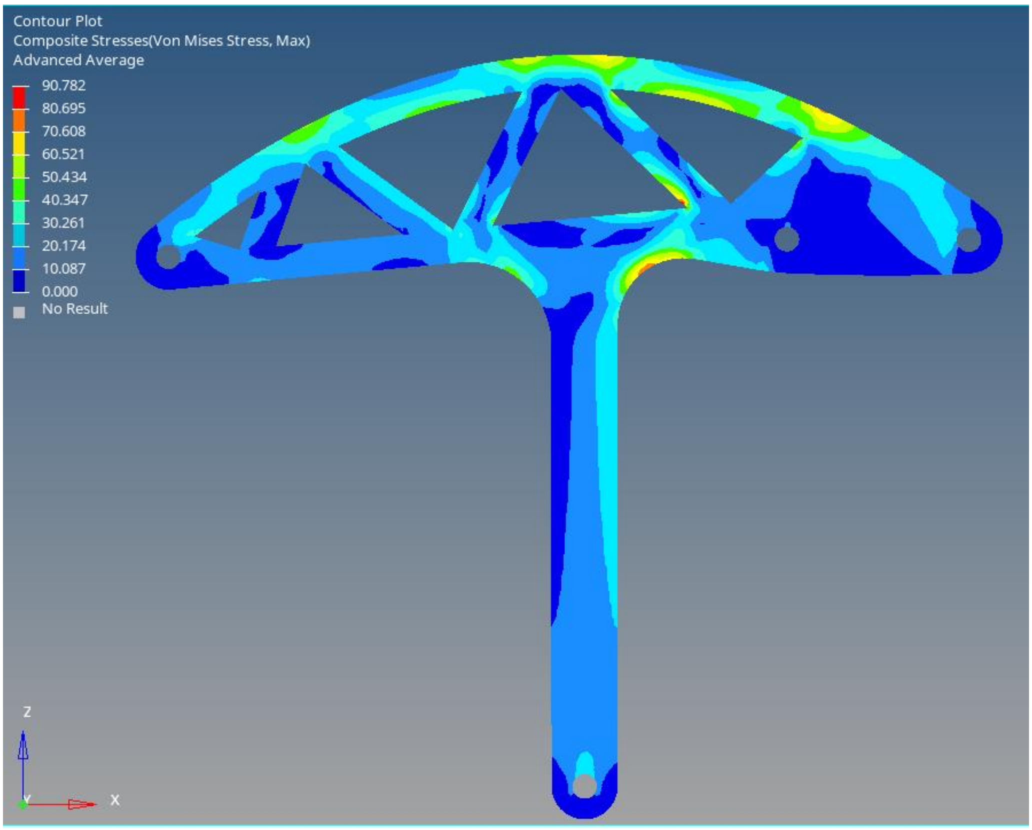

Figure 69. Support - Aerodynamic load stress

6.2 Technical regulations

200N distributed load

With a dimensioning based on the aerodynamic load, all components can easily be compliant with the technical requirements, as can be seen in next figures.
Unfortunately, this is not true for the beamwing. This happens because, differently from the flaps that are too inclined with respect to the horizontal, the sandbags can be placed on top of the element, therefore it must resist as well to this load case with satisfactory results. For what concerns the aerodynamic performance, 2 layers of carbon fibre are enough to achieve the desired target. However, if we look at the displacement generated by the 200 N load, 14.6 mm are obtained. Therefore, a configuration with 4 plies is adopted, with a resultant displacement of 6.4 mm, to have a safety margin from the maximum 10 mm imposed by the regulations.

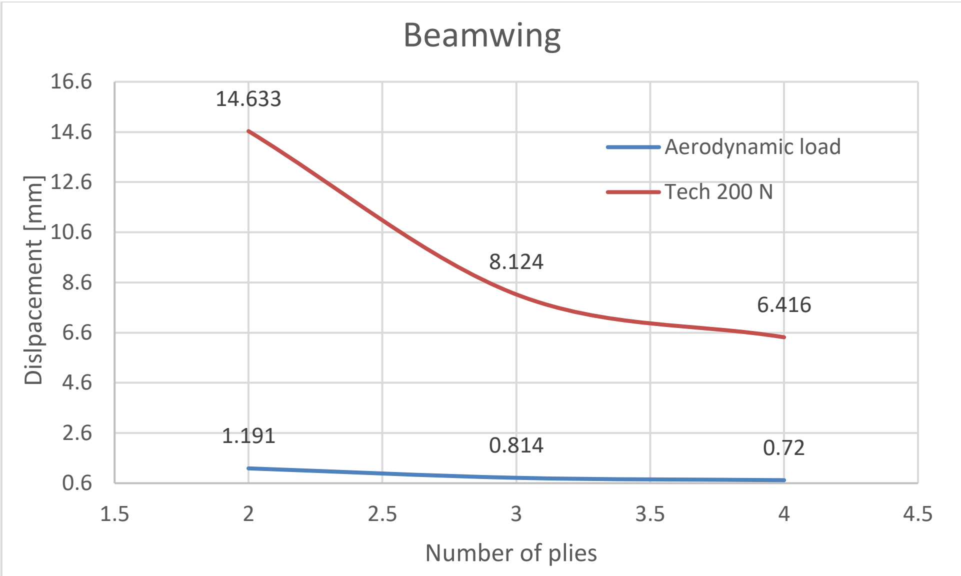

Figure 70. Beamwing displacement under 200 N distributed load

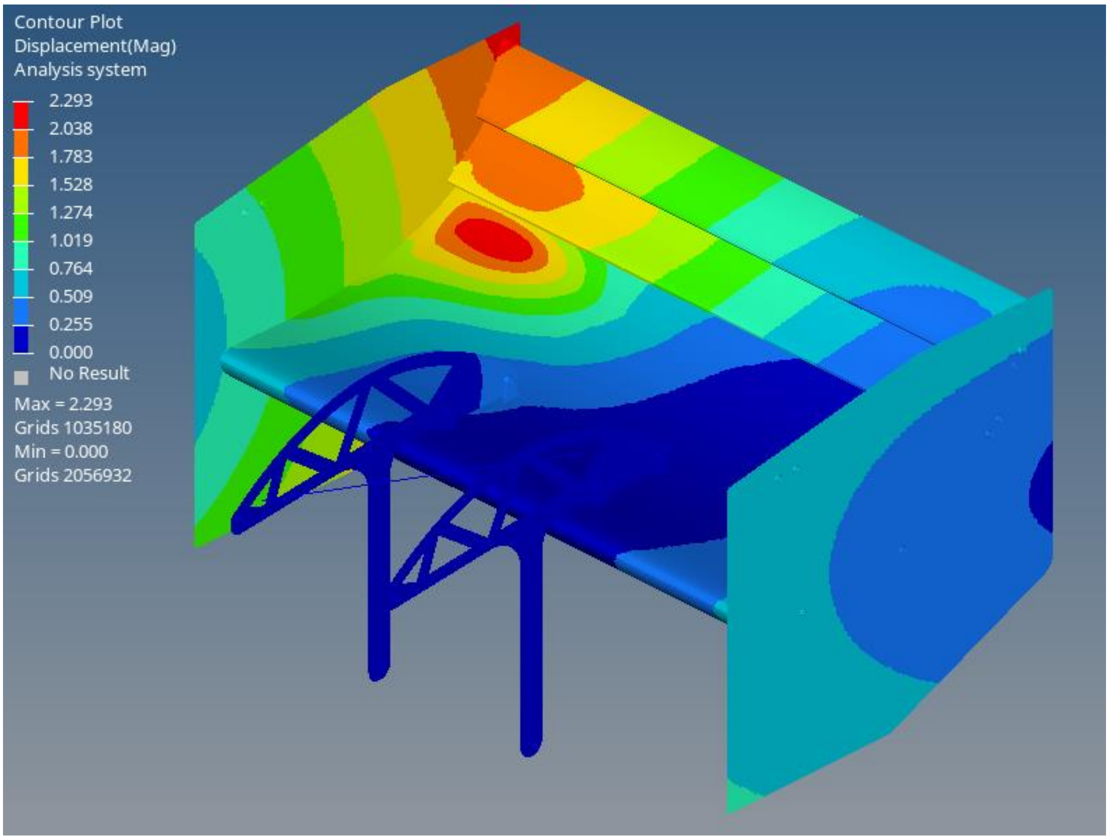

Figure 71. Rear Wing - 200N distributed load (on mainplane and flap 1) displacement

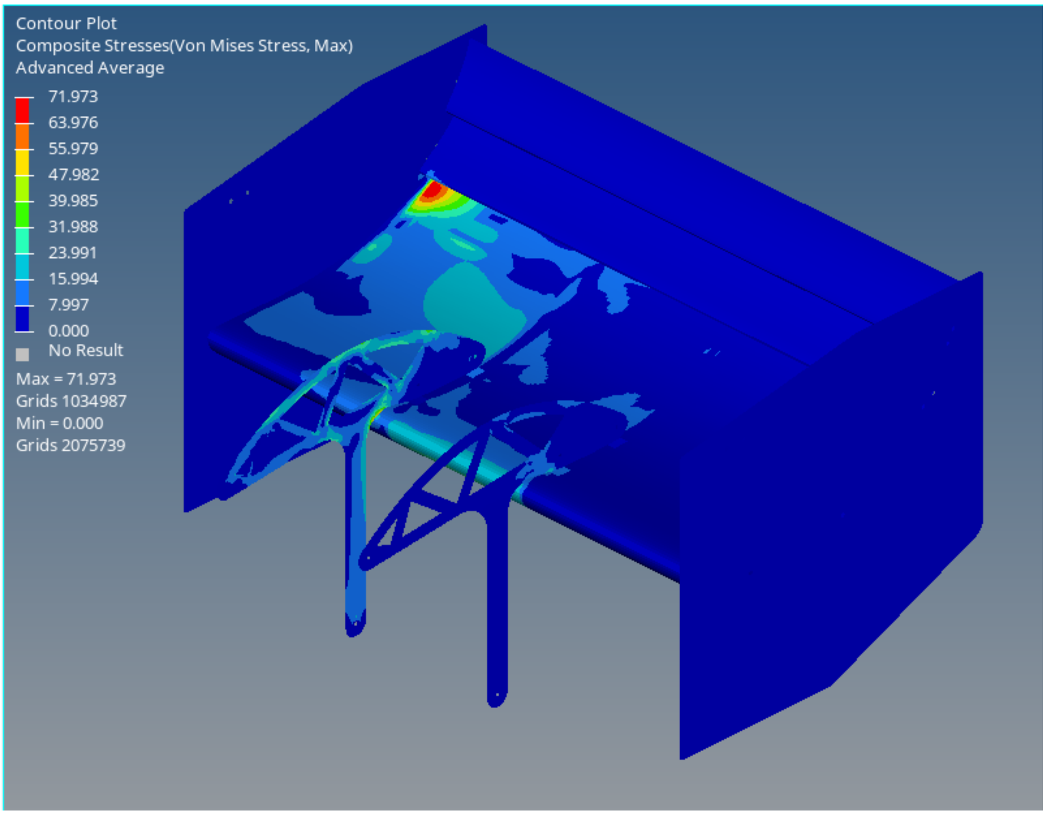

Figure 72. Rear Wing - 200N distributred load (on mainplane and flap 1) Stress

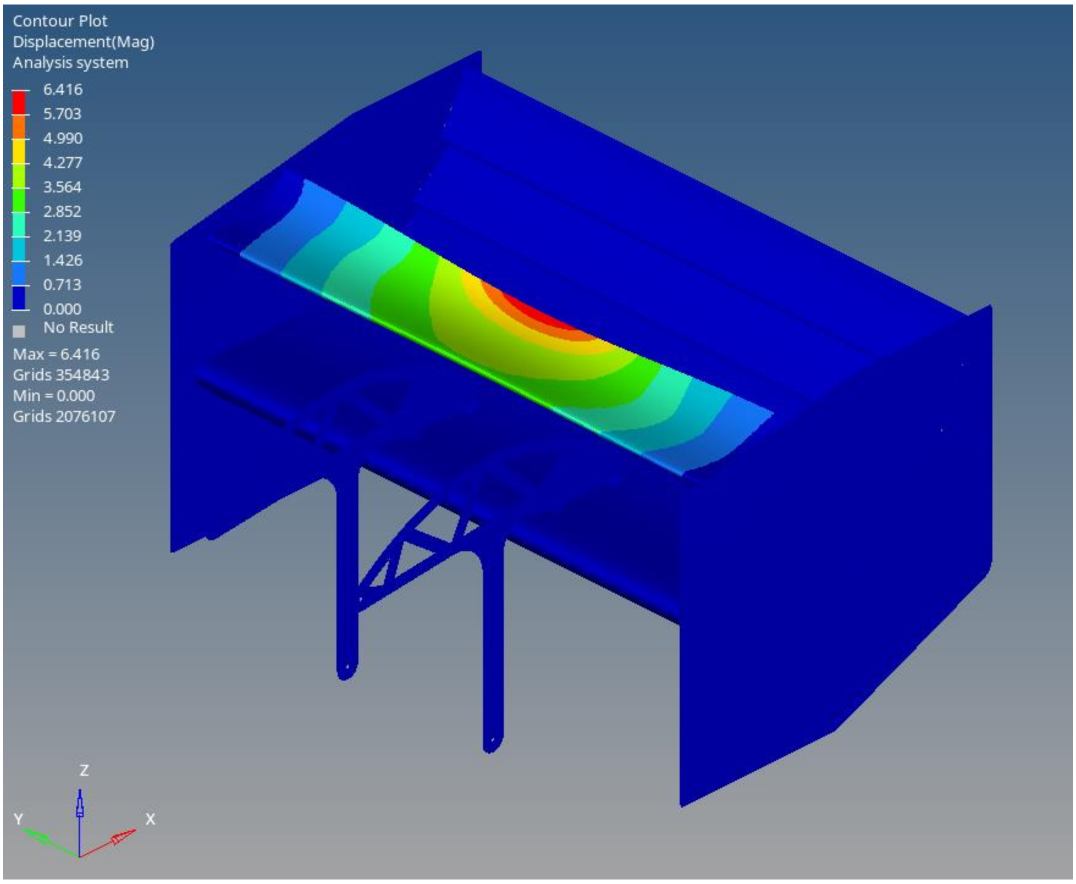

Figure 73. Rear Wing - 200N distributed load (on beamwing) Displacement

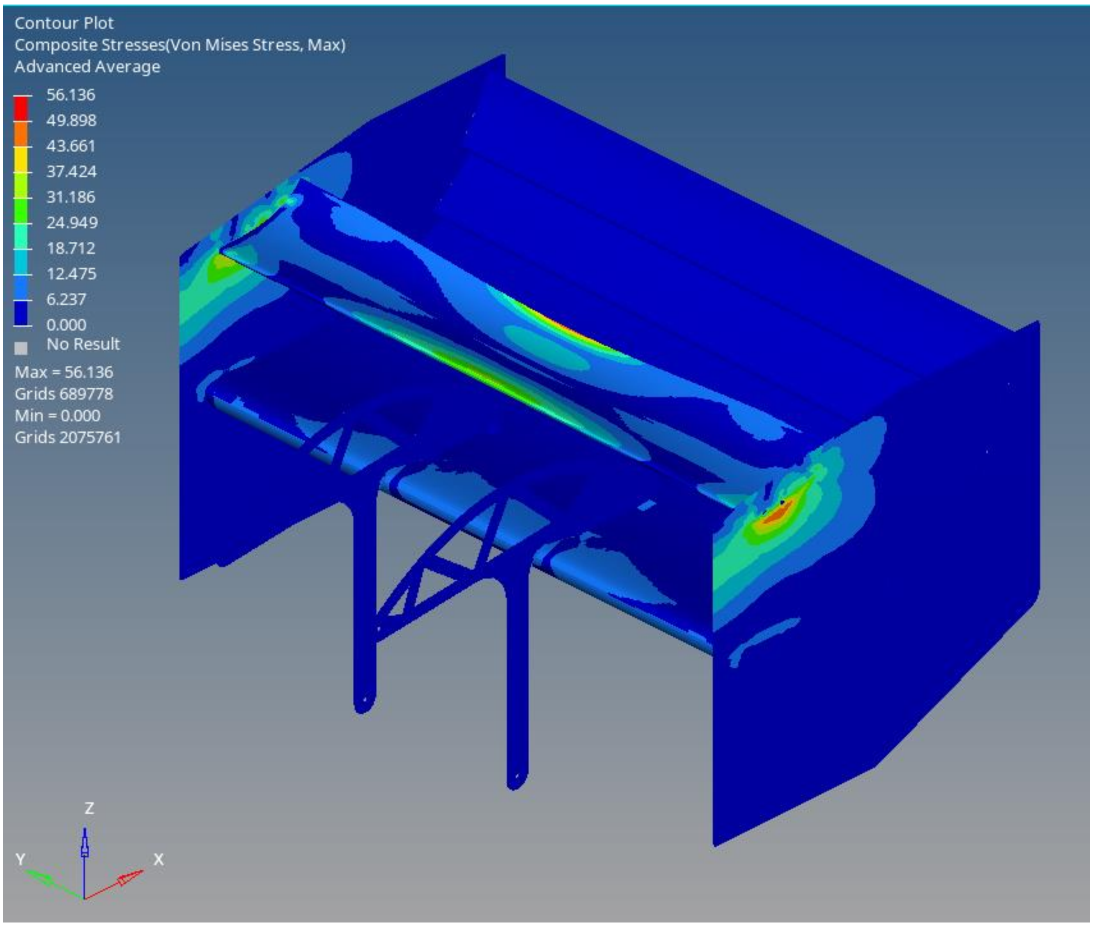

Figure 74. Rear Wing - 200N distributed load (on beamwing) Stress

50N

The 50 N technical regulation is easily verified for all components, since the maximum allowed displacement is of 25mm.

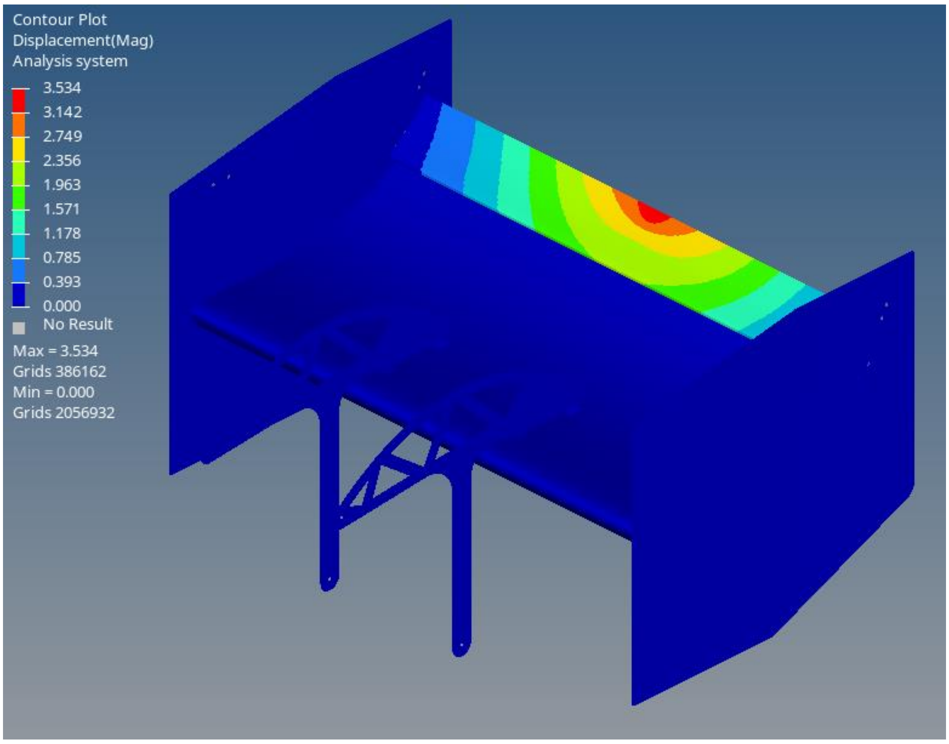

Figure 75. Flap 1 - 50N concentrated load displacement

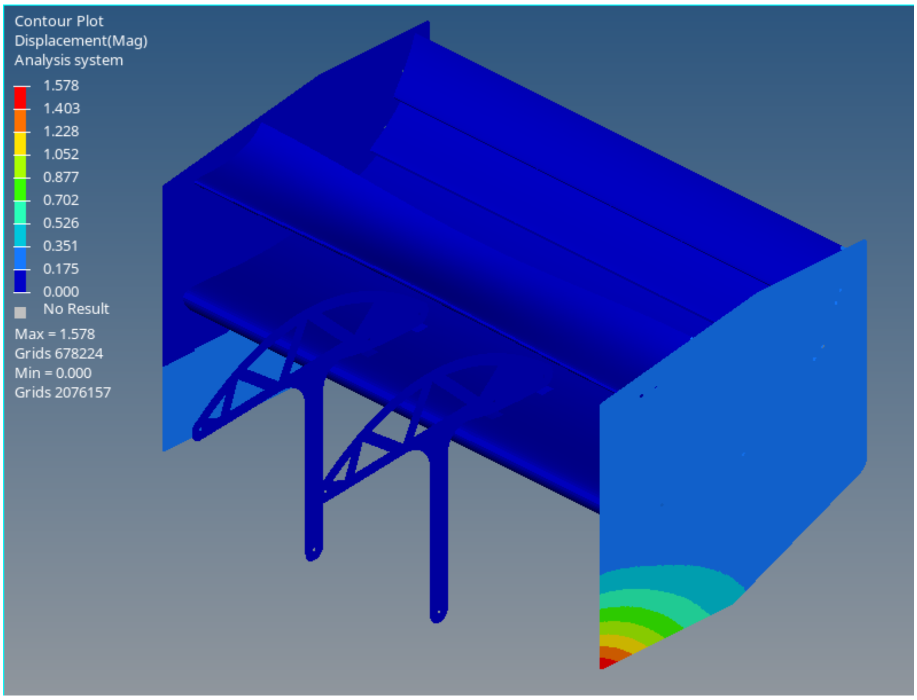

Figure 76. Endplate - 50N concentrated load displacement

6.3 Lateral load

Lateral load cases are less heavy than the aerodynamic one, nevertheless they are verified to check that no failure in the component would occur. In both cases, no failure occurs and the maximum stresses are far beyond the material strength.

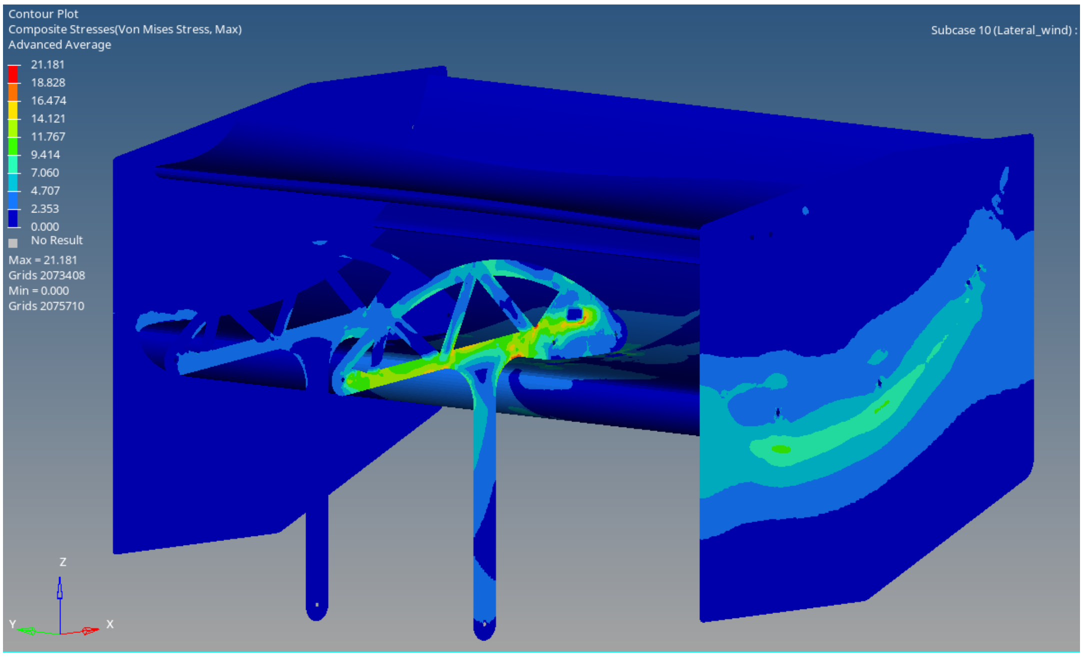

Figure 77. Endplate - 120km/h lateral wind stress

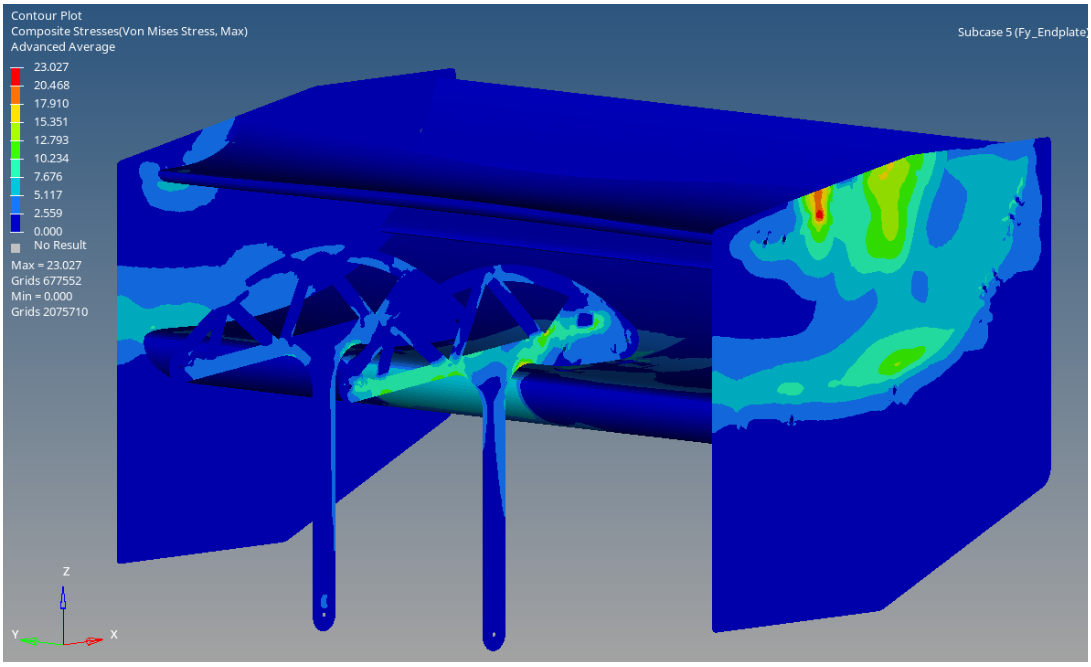

Figure 78. Endplate - 150N concentrated force stress

6.4 Longitudinal Force on Flap 2

The objective of this load test is to assess the structural integrity of the system under a specific load condition. The simulation replicates a scenario where an individual exerts force on the car improperly, pushing against the second flap of the rear wing. As can be seen by results scene, no failure of the components occurs.

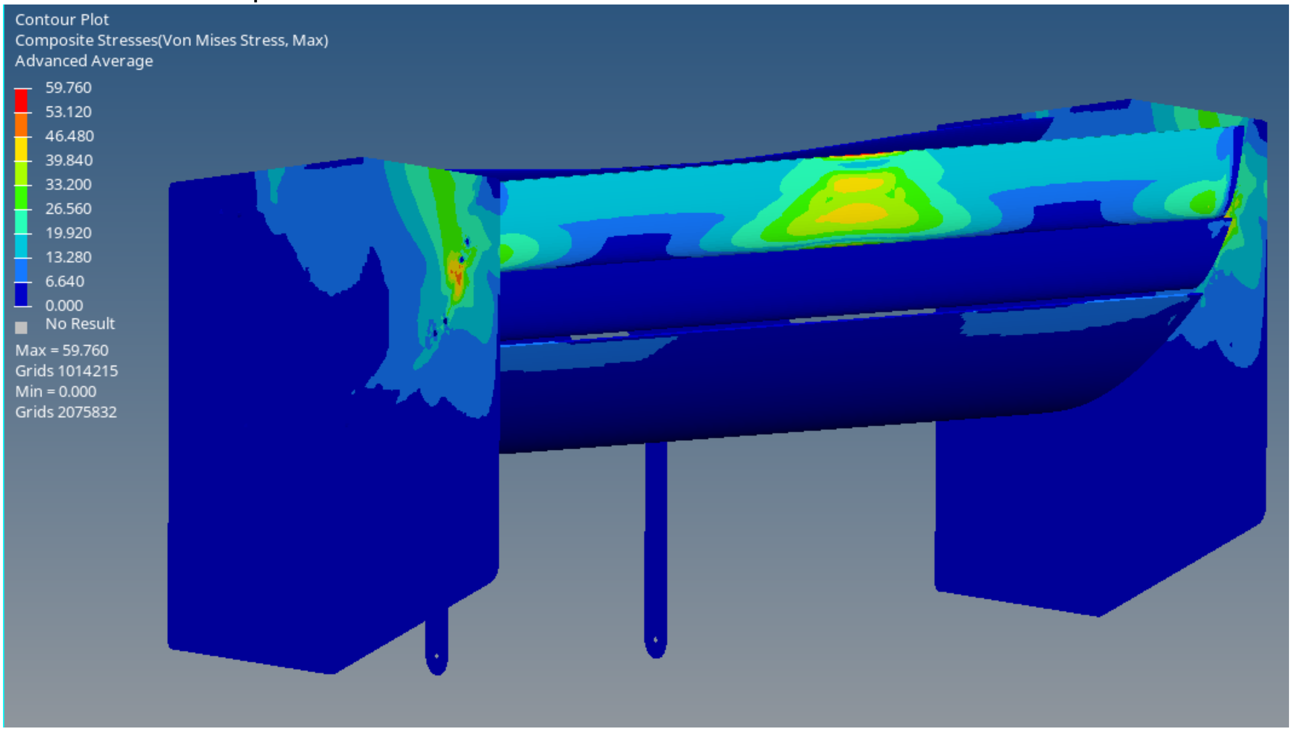

Figure 79. Flap 2 - 150N concentrated load stress

6.5 Calibrated bolts shear resistance verification

Calibrated bolts to mount the supports are over dimensioned on purpose, since they are not supposed to carry shear load and they are a crucial component for the structural integrity of the assembly. Shear resistance is verified according to the formula:

$$F_{s,MAX} = \frac{0.6 \cdot UTS \cdot A_{res}}{1.25}$$

Bolts of 8.8 class are used, therefore their ultimate tensile strength (UTS) is of 800 MPa. For an M5 bolt, the resistant section A_{res} is equal to 14.2 mm^2.
For this type of bolt is found a shear resistance of 5452 N.
From the simulations are obtained the constraint reaction acting on the bolts, for which the following results are obtained:

Bolt	Constraint force [N]
Rear Right	885
Front Right	365
Rear Left	950
Front Left	504

Table 20. Calibrated Bolt Constraint Reaction

Considering the mot loaded bolt, with a resultant force of 950 N, a safety factor of 5.7 is obtained.

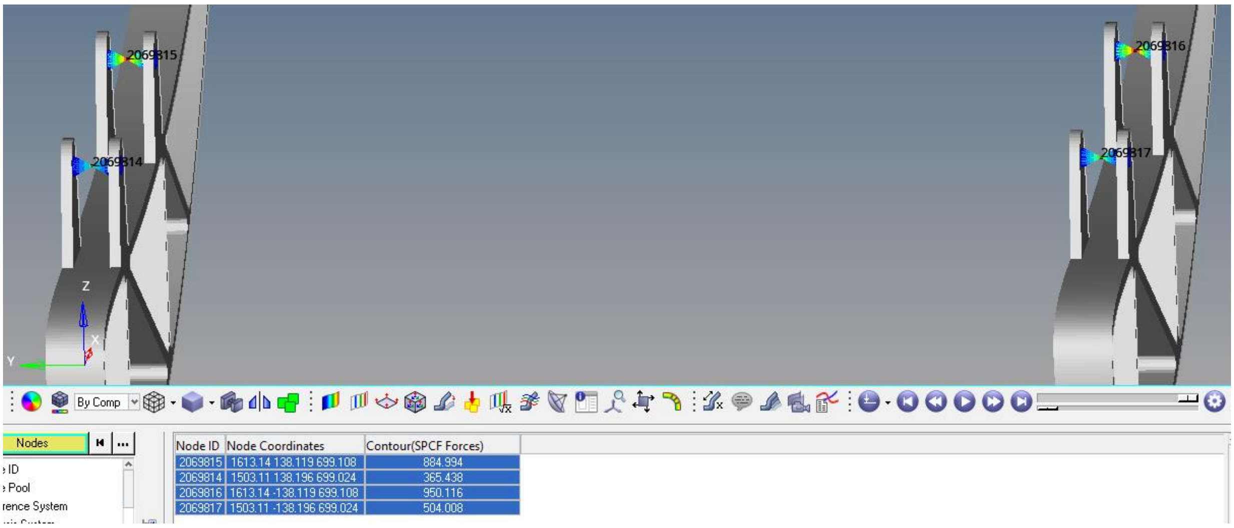

Figure 80. Constraint reaction - Aerodynamic load

6.6 Summary

The relevant results of displacement and stress over the analysed load cases are presented in the tables below. As can be seen, the stresses are generally low, with high values of safety factor. This is the result of the high stiffness required for these components to ensure their correct functioning.

Component	Displacement [mm]				
	60 km/h	90 km/h	120 km/h	Tech 200 N	Tech 50 N
Mainplane	0.604	1.345	2.423	2.293	/
Flap 1	1.617	3.636	6.504	/	3.534
Flap 2	1.501	3.396	6.089	/	/
Beamwing	0.72	1.632	2.931	6.416	/
Endplate	-	/	/	/	1.578

Table 21. Rear Wing 2024 Displacement result summary

Component	Stress [MPa]				
	120 km/h	Tech 200 N	Tech 50 N	Lateral laod	Longitudinal force
Mainplane	53.074	71.973	/	8.308	
Flap 1	26.824	12.234	45.214	2.365	
Flap 2	19.448	1.668	/	2.278	59.76
Beamwing	9.634	50.653	/	5.521	
Endplate	36.812	12.231	22.162	23.072	49.712
Support	90.958	57.325	/	17.911	10.592

Table 22. Rear Wing 2024 Stress results summary

7. Conclusions

In this chapter, the outcomes derived from the discussions in Chapter 6 are presented. The final laminate configuration and estimated weight of various components are detailed. It is noteworthy that the weight indicated for the support and endplate refers to a single piece and not the pair.

The tables below highlight a 4.5% reduction in weight for the Rear Wing Structure designed for the 2024 season compared to the 2021 assembly. Despite this weight reduction, the aerodynamic forces it must withstand have increased by 30%, emphasizing the effectiveness of the hollow and sandwich structure technique over the previous full-core rigid foam solution.

It's noteworthy that although the mainplane appears heavier than the 2021 version, the real weight of the 2021 component is 1.555kg (as indicated in Table 6), influenced significantly by the glue used for joining the core and outer shell. In the case of the 2024 component, this effect is expected to be much smaller, as the only components glued are the ribs, which have a considerably smaller interface surface.

The endplates for the 2024 assembly are crafted from prepreg carbon fibre, offering enhanced process control, and achieving two components with the same weight, resulting in an overall improved weight balance.

The most significant weight improvement is observed in the supports, thanks to their design focused on structural performance rather than aerodynamics, resulting in a component that is 56% lighter than its previous version.

COMPONENT	Nº PLIES	FIBRE	CORE	LAYUP	WEIGHT [kg]
Main	3	160gsm 5HS	Nomex	0º-45º	0.571
Flap 1	3	220gsm Twill	ROHACELL IG31	0º-45º	0.262
Flap 2	3	220gsm Twill	ROHACELL IG31	0º-45º	0.262
Beam	4	220gsm Twill	ROHACELL IG31	0º-45º	0.495
Endplate	2	160gsm 5HS	Nomex	0º-45º	0.392
Support	9	160gsm 5HS	Nomex	0º-45º	0.194

Table 23. Rear Wing 2024 laminates configuration

Ribs	**Material**	**Weight [kg]**	***Inserts***	**Material**	**Weight [kg]**
Main	Al 6060 T6	0.246	Supports	CFRP	0.034
Flap 1	Al 6060 T6	0.036	Endplates	CFRP	0.036
Flap 2	Al 6060 T6	0.036			
Beam	Al 6060 T6	0.044			
Main-Support	Al 6060 T6	0.51			

Table 24. Rear Wing ribs and inserts weight

Components	Estimated Weight [kg]		
	RW 2021	RW 2024	Difference %
Main	0.9196	1.327	44.3
Flap 1	0.496	0.298	-39.9
Flap 2	0.301	0.298	-1.0
Flap 3/Beam	0.349	0.539	54.4
Support	0.9568	0.422	-55.9
Endplate	0.8554	0.82	-4.1
Total	**3.8778**	**3.704**	**-4.5**

Table 25. Rear wing 2021 and Rear Wing 2024 comparison

Components	RW 2021		RW 2024	
	Downforce [N]	Drag [N]	Downforce [N]	Drag [N]
Main	315	9	670.16	149.48
Flap 1	126	43	101.42	108.7
Flap 2	136	111	42.02	104.84
Flap 3	57	95	/	/
Beam	/	/	80.02	14.12
Total	634	258	890.94	387.24
Resultant	684.49		971.46	
Difference	/		**+29.54%**	

Table 26. RW 21 vs RW 24 aerodynamic force comparison

Experimental test conduction and further development of it

The conduction of the experimental test is left for a future development of the analysis performed in this work. Further refinement can be done to the test, so that this can be reflected to an improvement of the reliability of the numerical model employed for the structural analysis of the aerodynamic assembly.

Bibliography

[1] Formula Student Germany. (2023). *Formula Student Rules 2024*. FSG.
[2] American Society for Testing and Materials. (2022). *Standard Test Method for Tensile Properties of Polymer Matrix Composite Materials (D3039)*. ASTM.
[3] Madler Dominique (2020). *Practical Finite Element Analysis for Mechanical Engineers.* FEA Accademy
[4] Katz Joseph (2006). *Race Car Aerodynamics*: *Design for Speed*. Bentley Publishers.
[5] Mallick, P. K. (2008). *Fiber-Reinforced Composites*: *Materials, Manufacturing, and Design.* CRC Press.
[6] Juvinall, R. C., & Marshek, K. M. (2011*). Fundamentals of Machine Component Design*. John Wiley & Sons.